An Investigation into the Capabilities of Three Simulation Tools for Small-Disturbance Stability Analysis

Prepared by:

Ntombela M.

MSc. Student

Department of Electrical Engineering

University of Cape Town

Prepared for:

The Department of Electrical Engineering

University of Cape Town

Thesis submitted in partial fulfilment of the requirements towards a Master of Science in Electrical Engineering degree in Electrical Engineering at the University of Cape Town.

22 May 2007

ACKNOWLEDGEMENTS

The author would like to thank the following people for their contribution towards the successful completion of this thesis:

- My supervisor Professor KA Folly, Department of Electrical Engineering – University of Cape Town for his continued support and guidance
- Professor AI Petroianu at the University of Cape Town for his continued support and guidance
- Professor Graham Rogers at Cherry Tree Scientific Software for his continued support with the two MATLAB packages used
- Dr Keren Kaberere at University of Cape Town for her continued support and guidance during the research.

The author also thanks friends, family and colleagues for their motivation and support towards the completion of this thesis.

DECLARATION

1. I know that plagiarism is wrong. Plagiarism is to use another's work and to pretend that it is ones own.

2. I have used the convention for citation and referencing. Each significant contribution to, and quotation in, this essay/report/project/... from the work, or works, of other people has been attributed, and has cited and referenced.

3. This thesis is my own work.

4. I have not allowed, and will not allow, anyone to copy my work with the intention of passing it off as his or her own work.

Ntombela M.

NTMMPU001

Signature.....

SYNOPSIS

"*Power system stability is that property of a power system that enables it to remain in a state of equilibrium under steady state operating conditions and to regain an acceptable state of equilibrium after being subjected to a disturbance.*" [1].

Small-disturbance stability is the ability of a power system to remain in a state of equilibrium under steady state operating conditions and to regain an acceptable state of equilibrium after being subjected to a small disturbance [1], [2]. There are several forms of small-disturbance stability as discussed in [1] and [2] for example, small-disturbance voltage stability. However, this thesis is concerned with small-disturbance angle stability, which is the ability of the system to maintain synchronism when subjected to small disturbances such as small variations in loads and generation [1], [2].

In large power systems, it is difficult to conduct field experiments hence, simulation tools are extensively used to investigate the stability of power systems. Power system planning and operation decisions rely to a large extent on the results obtained from these simulation tools. Therefore there is a need for researchers to investigate the capabilities of power system simulation tools. This MSc thesis forms part of more comprehensive research being conducted at the University of Cape Town comparing power system simulation tools. Part of the ongoing research at the University of Cape Town, which looks at solution methodology, power system component models and software flexibility using simulation tools not discussed in this thesis can be found in [4] and [7]. The objectives of this research are to investigate the capabilities of three power system simulation tools for small-disturbance angle stability analysis, namely PST, MatNetEig and CPAT

Computers today have become fast, efficient with high memory capacities and advanced in data processing capabilities. Many power system simulation tools are available on the market and making a decision about which simulation tool to purchase has become complicated, especially with existing high competition between vendors. Once a decision has been made and the tool has been purchased, most users do not want to change to a new tool for several reasons. Firstly, learning how to use power system simulation tools is time consuming and secondly, the tools are very expensive.

Investigating the capabilities of power system simulation tools for the different aspects of power system analysis will save power system planning and operation engineers and other

users time and money because they will know the capabilities of a tool before they purchase it.

A literature survey was conducted on the fundamentals of small-disturbance angle stability to investigate the important concepts involved in a small-disturbance stability analysis for the proper use of the tools.

A power system is a dynamic system because the state of a power system changes all the time. Dynamic systems can be expressed by nonlinear differential equations. However, for small-disturbance stability analysis, the nonlinear differential equations are linearized around the operating point. A disturbance is considered small if it is acceptable to linearize the nonlinear equations for the purpose of analysis. With the power system dynamic equations linearized, it is easy to used linear analysis methods in power systems.

There are several methods for small-disturbance stability analysis. These include methods in the time domain; methods in the frequency domain, such as the eigenvalue method and load flow methods such as methods derived from a Jacobian matrix, [12]. However, what is known as the eigenvalue technique has proved to be very useful in power systems. The eigenvalue technique is useful in that the nature of the eigenvalues gives valuable insight into the small-disturbance stability of the system for the operating point about which the linearisation was performed. The eigenvalue analysis technique for small-signal stability is discussed in this thesis because of its versatility and all three of the simulation tools investigated use the eigenvalue technique to analyse the stability of the system.

The literature revealed that when investigating small-disturbance stability, there are three important variables that can be used as performance measures. These are the *eigenvalues* and their associated *eigenvectors (right and left),* and the *participation factors*.

Eigenvalues give valuable information about the damping and the frequency of oscillatory modes in a system. The real part of eigenvalues gives the damping of the mode and the imaginary part gives the frequency of the oscillation. If the eigenvalues indicate a poorly damped oscillatory mode, it means that following a small-disturbance the power system may experience oscillations of growing amplitude, which may result in loss of synchronism. Participation factors are used to find the states of the system actively participating in an oscillatory mode.

The capabilities of the three simulation tools were investigated using two system models,

a single machine infinite bus system and a two-area, four-generator system taken from [1]. MATLAB PST was found to be only capable of handling small systems of up to 200 states; this is because MATLAB does a full modal analysis, which is very limited in the amount of data it can handle. PST lacks modelling flexibility and there are very few pre-programmed IEEE standard models (only three standard IEEE exciter models). Since PST is a MATLAB toolbox, it comes with the advantage that with MATLAB, system variables are easily accessible and the mathematical capabilities of MATLAB are quite good. To deal with the limitations of PST, Cherry Tree Scientific Software, the vendor of MATLAB PST developed another tool called MatNetEig also a MATLAB toolbox.

Since MatNetEig can perform partial modal analysis as well as full modal analysis, it can handle very large systems up to over 1000 states. Furthermore, MatNetEig has a better library of standard IEEE models. MatNetEig, however, is a toolbox designed particularly for linear analysis of power systems; unlike PST, it cannot perform transient stability simulations.

Neither package has a graphical user interface at the level of the sophisticated industrial grade packages, on which the user can input data by clicking on the different components on the network diagram. The two packages can, however, perform step response simulations which are small-disturbance time domain simulations.

CPAT is a power system analysis tool that was developed by the Central Research Institute of Electric Power Industry (CRIEPI) for the assessment of bulk power systems [37]. CPAT comprises three modules; the L-Method, the Y-Method and the S-Method. The L-Method is used to run power flow, the Y-Method is used to perform the nonlinear transient stability and the S-Method is used to perform small-disturbance stability simulations [37]. Unlike PST and MatNetEig, CPAT does have a graphical user interface. However, the user has to input all the power system data into notepad files. When inputting data, the user has to make sure that the column positions used are as specified in the manual, much more like the FORTRAN programming language. After inputting the system data, the user can draw a network diagram and then the system data input from notepad can then be linked to the network diagram. For small-disturbance stability analysis, CPAT can handle systems of up to 300 generators, 1500 nodes and 1800 branches. The program is capable of doing participation and eigenvectors, however, due to the fact that the user license was acquired at the final stages of the research, only the

eigenvalues could be calculated. The user manual of CPAT is not as easy to read as that of the other two packages. This may be because the manual was translated from Japanese to English, so it is possible that some of the data may have been twisted or is not as clearly put as it should be.

LIST OF FIGURES

LIST OF TABLES

TABLE OF CONTENTS

CHAPTER 1
INTRODUCTION

1.1 POWER SYSTEM STABILITY, TERMS AND DEFINITIONS

"Power system stability is that property of a power system that enables it to remain in a state of equilibrium under steady state operating conditions and to regain an acceptable state of equilibrium after being subjected to a disturbance" [1].

According to the recently published (May 2004) *"Definition and Classification of Power System Stability"* paper [2] by the *IEEE/CIGRE Joint Task Force on Stability Terms and Definitions* there are three main categories of power system stability, which are:

1. Rotor angle stability
    a Small-disturbance angle stability (Short term)
    b Transient stability (Short term)
2. Frequency stability
    a (Short term)
    b (Long term)
3. Voltage stability
    a Large-disturbance voltage stability (Short / long term)
    b Small-disturbance voltage stability (Short / long term)

Short term implies the period of interest following a disturbance is in the order of seconds, typically 10 to 20s. Long term implies the period of interest following a disturbance ranges from several to many minutes.

Rotor angle stability is the ability of synchronous machines of an interconnected power system to remain in synchronism after being subjected to a disturbance. Small-disturbance rotor angle stability is the ability of the system to maintain synchronism when subjected to small disturbances, such as small variations in loads and generation [1], [2]. Transient stability is the ability of a power system to maintain synchronism when subjected to a

severe transient disturbance, such as a short circuit on a transmission line [1], [2]. The scope of this research is restricted to rotor angle stability, particularly small-disturbance rotor angle stability. Power systems are dynamic nonlinear systems whose behaviour can be described by nonlinear ordinary differential equations [1]. A disturbance is considered small if linearization of the nonlinear system equations is acceptable for the purposes of analysis [1], [2].

Small-disturbance rotor angle stability can be further classified into two forms [1], [2]:

1. Steady increase in rotor angle due to lack of sufficient synchronizing torque
2. Rotor oscillations of increasing amplitude due to lack of sufficient damping torque

1.2 BRIEF HISTORICAL OVERVIEW OF POWER SYSTEM STABILITY

The power system stability problem is not new in power systems. Historically, transient stability has been the dominant stability problem on most power systems and thus has been the focus of industry's attention [2], [9]. In the past, many utilities took small-disturbance stability for granted and they depended on transient stability simulations to reveal problems related to small-disturbance performance [9]. Over time, power systems have evolved through continuing growth in interconnections, use of new technologies and controls, and increased operation in highly stressed conditions. Different forms of instability have been observed, with small-disturbance angle stability being one of them [2].

Modern power system generators are equipped with continuously fast-acting automatic voltage regulators, which greatly improve synchronizing torque following a transient disturbance [1], [2], [8]. The small-disturbance angle stability problem is largely that of insufficient damping of oscillations [1], [2], [8].

The eigenvalue technique for analysing the small-disturbance performance of a power system is a powerful technique [2], [10]. The three simulation tools investigated in this thesis, PST, MatNetEig and CPAT all use the eigenvalue technique but take different approaches to the calculation of eigenvalues and the modelling of power system components.

1.3 JUSTIFICATION OF THE RESEARCH

Over time, computers have become fast and efficient, with high memory capacities and advanced in their data processing capabilities and many power system simulation tools have become available in the market. Making a decision about which simulation tool to purchase has become complicated, especially with the existing high competition from vendors. For many engineers, learning new power system simulation tools is time consuming. In addition, these tools are very expensive. Investigating the capabilities of power system simulation tools for the different aspects of power system analysis will save time and money for power system planning and operation engineers and other users. This thesis investigates the capabilities of the three power system simulation tools, MATLAB Power System Toolbox (PST), MATLAB MatNetEig and CRIEPI's Power System Analysis Tool (CPAT).

1.4 OBJECTIVES

The objectives of the research were to investigate the capabilities of the three power system simulation tools for small-disturbance angle stability analysis by:

- Investigating small-disturbance angle stability in power systems
- Investigating the primary objective(s) and procedure for carrying out a small-disturbance angle stability analysis in power systems
- Investigating the various factors affecting results obtained from a small-disturbance analysis
- Formulating and performing case studies.

1.5 METHODOLOGY

The research was conducted as follows:

1.5.1 Literature survey

In the early stages of the research, an extensive literature survey on power system small-disturbance angle stability was conducted.

1.5.2 Learning PST and MatNetEig

The second stage of the research was learning the two MATLAB simulation tools PST and MatNetEig. Learning how to use the two simulation tools was time consuming, largely because of the way the data is inputted in the two simulation tools. There is no graphical representation of the network where the user can easily input data on each component but data is inputted in matrices. However, G.J. Rogers who is part of Cherry Tree Scientific Software, the vendor for the two simulation tools and author of the book *"Power System Oscillations"* [8], gave the author invaluable guidance into the use of PST and MatNetEig for small-disturbance angle stability analysis.

1.5.3 Investigating the capabilities of PST and MatNetEig

The next stage was to investigate the capabilities of PST and MatNetEig for small-disturbance angle stability analysis by looking at:

1. Modelling capabilities
2. Approach to the solution methodology
3. Flexibility/ease of use i.e. input/output data
4. Special features, if any.

To look at the above-mentioned 1-4, case studies were carried out by using both the single machine infinite bus system and the two-area four-generator system.

1.5.4 Case Studies

The following case studies were carried out in the investigation of the capabilities of the simulation tools:

1. The single machine infinite bus system:

    - System under manual control with synchronous generator modelled with

the classical model

- System under manual control with synchronous generator modelled with the sixth order model
- System with synchronous generator modelled using the sixth order model equipped with an excitation system with automatic voltage regulation
- System with synchronous generator modelled using the sixth order model equipped with an excitation system with automatic voltage regulation and a power system stabilizer

2. The two-area four-generator system

- System is under manual control. Generators are modelled using the sixth order model
- All four generators are modelled with the sixth order model and are now equipped with similar excitation systems with automatic voltage regulation
- All four generators are modelled with the sixth order model and are now equipped with similar excitation systems with automatic voltage regulation and power system stabilizers

These case studies were carried out to see if the tools can reveal the small-signal stability of the system when various factors are taken into consideration.

1.5.5 Inputting data into PST and MatNetEig

The next stage was to input data into PST and MatNetEig for the two test systems to be used. The single machine infinite bus system and the two-area four-generator system obtained from chapter 12 of [1] were the two systems chosen for investigating the capabilities of simulation tools for small-disturbance angle stability analysis. Results obtained were compared with those obtained using other simulation tools and those found in the literature [1]. Some of the results were published in [4], [5], [6], [7]. To verify the frequency domain results, step-response simulations were also carried out.

1.6 CONTRIBUTIONS OF THIS THESIS

This thesis investigates:

- the capabilities of the three software tools (e.g., PST, MatNetEig and CPAT) for small-signal stability analysis
- the user friendliness of each tool
- the limitations of the tools for performing small-disturbance stability analysis.

1.7 LIMITATIONS OF THE RESEARCH

There are some important aspects in small-disturbance stability analysis that are beyond the scope of this thesis. These include the effect of modelling generator magnetic saturation in small-signal stability. This research was limited to studying the small-disturbance stability of two benchmark systems taken from [1].

1.8 THESIS OUTLINE

Chapter 2 lays the foundation of the fundamental aspects of small signal stability.

Chapter 3 discusses the way small signal stability analysis is carried out, and the important aspects in the prediction of a small signal stability of a power system.

Chapter 4 discusses the modelling of power system components in stability.

Chapter 5 discusses the capabilities of MATLAB PST for small signal stability analysis.

Chapter 6 discusses the capabilities of MATLAB MatNetEig for small signal stability analysis.

Chapter 7 discusses the capabilities of CRIEPI Power System Analysis Tool (CPAT) for small signal stability analysis.

Chapter 8 presents the system models that are used in the case studies conducted and the case studies that were conducted with the three simulation packages.

Chapter 9 gives the conclusions and recommendations based on the case studies carried out.

CHAPTER 2
Overview of Small-Disturbance Angle Stability

The basic terms and definitions in small-disturbance stability have been briefly discussed in chapter 1. This chapter gives an overview of the mathematical representation of a power system in small-disturbance stability, the characteristics of synchronous machines and their effect on small-disturbance stability and the linearization of system equations leading to the computation of eigenvalues and eigenvectors in small-disturbance stability.

2.1 INTRODUCTION

Section 2.2 of this chapter presents an overview of stability. Section 2.3 discusses the synchronous machine characteristics related to synchronous operation and the stability phenomena. Section 2.3 lays the foundation for the discussion of the behaviour of synchronous machines and their effect on small-disturbance stability. Section 2.4 discusses the mathematical representation of the power system in small-disturbance stability. Section 2.5 discusses the linearization of system equations. Section 2.6 discusses eigenvalues and eigenvectors in small-disturbance stability. Following the discussion of the fundamental aspects of small-disturbance stability, Section 2.7 presents the historical review of small-disturbance stability problems discussed in [1] and [8].

2.2 OVERVIEW OF POWER SYSTEM STABILITY

When a power system in steady-state is disturbed, the stability of the system depends on the initial operating condition as well as the nature of the disturbance [1], [2]. Power systems are subjected to a wide range of disturbances, such as small changes in load and generation, lightning strikes, short circuits etc. This makes the topic of stability in power systems very broad and there are thus different categories of stability. The different types of stability are classified according to[1]:

- *The physical nature of the resulting instability*
- *The size of the disturbance*
- *The devices, the processes and the time span that must be taken into consideration when determining stability*

- *The most appropriate approach to calculating and predicting stability*

Figure 2.1 is taken from [2] and it is a graphical illustration of the different categories of stability.

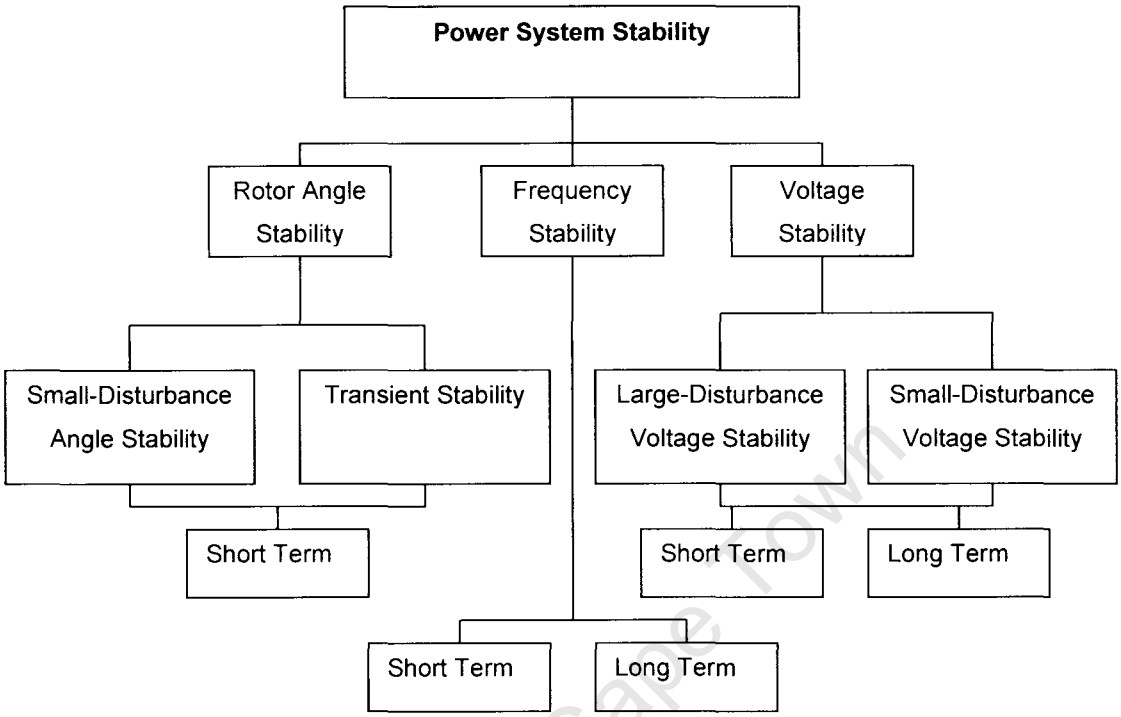

Figure 2.1: *Classification of power system stability (taken from [2])*

Rotor Angle Stability refers to the ability of synchronous machines in an interconnected power system to maintain synchronism after being subjected to a disturbance [1], [2].

Frequency Stability refers to the ability of a power system to maintain steady frequency following a severe system upset resulting in a significant imbalance between generation and load [1], [2].

Voltage Stability refers to the ability of a power system to maintain steady voltages at all buses in the system, both under normal operating conditions and after being subjected to a disturbance from a given initial operating condition [1], [2].

The first step when performing a stability study is to form a mathematical model of the system. Before a disturbance is introduced into the system, the operating state of the system obtained from the load flow solution must be known in order to initialise the mathematical models used to model the different power system components. Depending

on the type of stability being studied, the relevant analysis techniques are applied on the system model. The scope of this thesis restricts the discussion to small-disturbance angle stability. Small-disturbance angle stability is concerned with the behaviour of a synchronous machine after its equilibrium (when input mechanical torque matches the developed electrical torque) has been disturbed. The next section, therefore, presents synchronous machine characteristics associated with synchronous operation.

2.3 SYNCHRONOUS MACHINE CHARACTERISTICS

The synchronous generator comprises two basic elements, the field and the armature. Conventionally, the field is mounted on the rotor and the armature on the stator of the generator and the field is dc excited. In a generator, the rotor is driven by the prime mover, for example, a steam turbine. The field on the rotor cuts the stator windings as the rotor rotates inducing alternating voltages (and currents if the generator is connected to a load). The frequency of these voltages depends on the speed of the rotor.

"*The armature windings are distributed on the stator such that the induced alternating currents flowing in the three phase windings produce a rotating magnetic field, that under steady-state operation, rotates at the same speed as the rotor*" [1].

When the rotor and the stator fields interact, they tend to align. The torque that tries to align the two fields by opposing the rotation of the rotor field is known as the electromagnetic torque. In a generator, to keep the rotor rotating, mechanical torque must be applied to the rotor to turn it. Electricity is generated by the conversion of this mechanical power (torque) applied to the rotor.

When a generator generates electrical energy, there is always an angular separation between the two fields. The rotor field always leads the stator rotating field. When there is an increase in the power drawn from the generator, there is an increase in the electromagnetic torque. The effect of the increase in electromagnetic torque is to slow down the rotor. When generator controls (governor) sense a drop in frequency or rotor speed, they react by applying more torque to maintain the desired constant frequency (50Hz in South Africa). This increase in generator output increases the angular separation between the rotor field and the stator field. Therefore, on the one hand, the governor controls control the MW output of the generator and on the other hand, the AVR (Automatic Voltage Regulator) controls the voltage at the terminals of the generator and

reactive power flow.

The philosophy explained above describes how an isolated single generator connected to a load would behave. In an interconnected power system, however, the behaviour of synchronous machines is slightly different. When synchronous machines are interconnected, they are synchronized. There is an angular separation between the fields of the rotors of the interconnected machines. This angular separation determines how generators share the loads (MW). The governor droop settings of the generator determine the percentage of the load each generator will pick up depending on its capacity. If a generator increases its MW output, it runs faster than another and the angular position of its rotor field relative to that of the slower machine will advance. This angular separation transfers part of the load from the slower machine to the faster machine. The effect of this load transfer is to reduce the speed difference. In stability, the angular separation should not go beyond a certain limit.

"*For any given situation the stability of the system depends on whether or not the deviations in angular positions of the rotors result in sufficient restoring torques (synchronizing and damping torque which will be explained in the consequent sections)*" [1].

2.4 THE POWER SYSTEM

Electricity demand changes all the time and the state of the power system is also changing constantly. To maintain system stability, generation must always match demand plus system losses, thus a power system is a dynamic system. The following descriptions regarding the behaviour of dynamic systems are taken from [1], [11], [12].

"*The behaviour of dynamic systems may be described by n nonlinear ordinary differential equations of the form* [1], [11], [12]:

$$\dot{x}_i = f_i(x_1, x_2, \ldots, x_n; u_1, u_2, \ldots, u_r; t) \qquad i = 1,2,\ldots,n \tag{2.1}$$

where n is the order of the system and r is the number of inputs".

For brevity Equation (2.1) can be written in vector notation as follows [1]:

$$\dot{\mathbf{x}} = \mathbf{f}(\mathbf{x}, \mathbf{u}, t) \tag{2.2}$$

where:

$$\mathbf{x} = \begin{bmatrix} x_1 \\ x_2 \\ \vdots \\ x_n \end{bmatrix} \qquad \mathbf{u} = \begin{bmatrix} u_1 \\ u_2 \\ \vdots \\ u_r \end{bmatrix} \qquad \mathbf{f} = \begin{bmatrix} f_1 \\ f_2 \\ \vdots \\ f_n \end{bmatrix} \tag{2.3}$$

"When the behaviour of a dynamic system is modelled using the state space approach n linearly independent state variables are chosen. In Equation (2.3) the entries of the column vector $\mathbf{x}$ *referred to as the state vector are state variables* x_i*. These variables represent the minimal set of state variables that, along with the inputs to the system, provide a complete description of the system behaviour [1]. The state of the system given by* $\mathbf{x}$ *represents the minimum amount of information about the system at any given instant in time* t_0 *that is necessary to determine its future behaviour without reference to the input before* t_0 *[1]. The system state may be represented in an n-dimensional Euclidean space called the state space where changing the choice of state variables simply means choosing a different co-ordinate system [1]. State variables can be chosen anyhow, however the variables must be independent otherwise the system is over specified. "State variables may be physical quantities in a system such as angle, speed, voltage, or they may be abstract mathematical variables associated with the differential equations describing the dynamics of the system* [1]*. The column vector* $\mathbf{u}$ *is the vector of inputs* u_i *to the system. The column vector* $\mathbf{f}$ *is the vector of nonlinear functions relating state and input variables to the time derivatives of state variables* $\mathbf{x}$ *denoted by* $\dot{\mathbf{x}}$*"* [1].

"If the derivatives of the system state variables are not explicit functions of time, Equation (2.2) simplifies to "[1]:

$$\dot{\mathbf{x}} = \mathbf{f}(\mathbf{x}, \mathbf{u}) \tag{2.4}$$

"The output variables that can be observed on the system can be expressed in terms of state and input variables by the equation:

$$\mathbf{y} = \mathbf{g}(\mathbf{x}, \mathbf{u}) \tag{2.5}$$

where:

$$\mathbf{y} = \begin{bmatrix} y_1 \\ y_2 \\ \vdots \\ y_m \end{bmatrix} \qquad \mathbf{g} = \begin{bmatrix} g_1 \\ g_2 \\ \vdots \\ g_m \end{bmatrix} \tag{2.6}$$

The column vectors $\mathbf{y}$ *and* $\mathbf{g}$ *are vectors of output variables and m nonlinear functions relating state and input variables to output variables respectively* [1]".

The next section discusses how these differential equations are linearized for application in small-disturbance analysis.

2.5 LINEARIZATION

In small-disturbance stability, nonlinear differential equations may be linearized for the purpose of analysis [1]. In small-disturbance stability analysis, it is assumed that the system is initially operating in steady state and the equations are linearized about this operating point [1], [2], [11], [12]. A disturbance is considered small if the linearized equations describe the behaviour of the system with reasonable accuracy. In other words, "*a disturbance is considered to be small if the equations that describe the resulting response of the system may be linearized for the purpose of analysis*" [1].

When the power system is operating in steady state, it is said to be in equilibrium, i.e. when the system state $\mathbf{x}$ is not changing, and all the derivatives (all entries of $\dot{\mathbf{x}}$) are simultaneously zero [1]. Given that $\mathbf{x}_0$ is the state vector, and $\mathbf{u}_0$ is the input vector at the equilibrium point, Equation (2.4) becomes [1]:

$$\dot{\mathbf{x}}_0 = \mathbf{f}(\mathbf{x}_0, \mathbf{u}_0) = 0 \tag{2.7}$$

If the system is perturbed from its equilibrium state by letting $\mathbf{x} = \mathbf{x}_0 + \Delta\mathbf{x}$ and $\mathbf{u} = \mathbf{u}_0 + \Delta\mathbf{u}$ then [1]:

$$\dot{\mathbf{x}}_0 + \Delta\dot{\mathbf{x}} = \mathbf{f}[(\mathbf{x}_0 + \Delta\mathbf{x}), (\mathbf{u}_0 + \Delta\mathbf{u})] \tag{2.8}$$

Assuming that the perturbations applied to the system are small enough, the nonlinear function $\mathbf{f}$ in Equation (2.8) can be expressed in terms of a Taylor series expansion. Ignoring terms of second and higher order powers of $\Delta\mathbf{x}$ and $\Delta\mathbf{u}$ [1],:

$$\dot{x}_i = \dot{x}_{i0} + \Delta\dot{x}_i = f_i(\mathbf{x}_0, \mathbf{u}_0) + \frac{\partial f_i}{\partial x_1}\Delta x_1 + \cdots + \frac{\partial f_i}{\partial x_n}\Delta x_n + \frac{\partial f_i}{\partial u_1}\Delta u_1 + \cdots + \frac{\partial f_i}{\partial u_r}\Delta u_r \tag{2.9}$$

Since $\dot{x}_{i0} = f_i(\mathbf{x}_0, \mathbf{u}_0) = 0$, [1]:

$$\Delta\dot{x}_i = \frac{\partial f_i}{\partial x_1}\Delta x_1 + \cdots + \frac{\partial f_i}{\partial x_n}\Delta x_n + \frac{\partial f_i}{\partial u_1}\Delta u_1 + \cdots + \frac{\partial f_i}{\partial u_r}\Delta u_r \tag{2.10}$$

Likewise [1]:

$$\Delta y_k = \frac{\partial g_k}{\partial x_1}\Delta x_1 + \cdots + \frac{\partial g_k}{\partial x_n}\Delta x_n + \frac{\partial g_k}{\partial u_1}\Delta u_1 + \cdots + \frac{\partial g_k}{\partial u_r}\Delta u_r \tag{2.11}$$

where $i = 1,2,\ldots,n$ is the state number, similarly $k = 1,2,\ldots,m$ in (2.11) is the number of output, n is the number of state variables and r is the number of inputs.

The linearized forms of Equations (2.4) and (2.5) are then given by [1]:

$$\Delta\dot{\mathbf{x}} = \mathbf{A}\Delta\mathbf{x} + \mathbf{B}\Delta\mathbf{u} \tag{2.12}$$

$$\Delta\mathbf{y} = \mathbf{C}\Delta\mathbf{x} + \mathbf{D}\Delta\mathbf{u} \tag{2.13}$$

Where:

$$\mathbf{A}=\begin{bmatrix} \frac{\partial f_1}{\partial x_1} & \cdots & \frac{\partial f_1}{\partial x_n} \\ \cdots & \cdots & \cdots \\ \frac{\partial f_n}{\partial x_1} & \cdots & \frac{\partial f_n}{\partial x_n} \end{bmatrix} \qquad \mathbf{B}=\begin{bmatrix} \frac{\partial f_1}{\partial u_1} & \cdots & \frac{\partial f_1}{\partial u_r} \\ \cdots & \cdots & \cdots \\ \frac{\partial f_n}{\partial u_1} & \cdots & \frac{\partial f_n}{\partial u_r} \end{bmatrix}$$

$$\mathbf{C}=\begin{bmatrix} \frac{\partial g_1}{\partial x_1} & \cdots & \frac{\partial g_1}{\partial x_n} \\ \cdots & \cdots & \cdots \\ \frac{\partial g_m}{\partial x_1} & \cdots & \frac{\partial g_m}{\partial x_n} \end{bmatrix} \qquad \mathbf{D}=\begin{bmatrix} \frac{\partial g_1}{\partial u_1} & \cdots & \frac{\partial g_1}{\partial u_r} \\ \cdots & \cdots & \cdots \\ \frac{\partial g_m}{\partial u_1} & \cdots & \frac{\partial g_m}{\partial u_r} \end{bmatrix} \tag{2.14}$$

and

$\Delta\mathbf{x}$ is the state vector of dimension n.

$\Delta\mathbf{y}$ is the output vector of dimension m.

$\Delta\mathbf{u}$ is the input vector of dimension r.

$\mathbf{A}$ is the state matrix of dimension $(n\times n)$

$\mathbf{B}$ is the input matrix of dimension $(n\times r)$

$\mathbf{C}$ is the output matrix of dimension $(m\times n)$

$\mathbf{D}$ is the feedfoward matrix of dimension $(m\times r)$ which defines the proportion of input which appears directly in the output.

State Equation (2.12) and (2.13) can be obtained in the frequency domain by using the Laplace transform. A solution to the state equations can then be found as follows [1]:

$$\Delta\mathbf{x}(s)=\frac{adj(s\mathbf{I}-\mathbf{A})}{\det(s\mathbf{I}-\mathbf{A})}[\Delta\mathbf{x}(0)+\mathbf{B}\Delta\mathbf{u}(s)] \tag{2.15}$$

$$\Delta\mathbf{y}(s)=\mathbf{C}\frac{adj(s\mathbf{I}-\mathbf{A})}{\det(s\mathbf{I}-\mathbf{A})}[\Delta\mathbf{x}(0)+\mathbf{B}\Delta\mathbf{u}(s)]+\mathbf{D}\Delta\mathbf{u}(s) \tag{2.16}$$

where $\mathbf{I}$ is the identity matrix, *adj* is the adjoint matrix and *det* is the determinant.

The poles of $\Delta\mathbf{x}(s)$ and $\Delta\mathbf{y}(s)$ are the roots of Equation (2.17) [1]:

$$\det(s\mathbf{I} - \mathbf{A}) = 0 \tag{2.17}$$

The values of s, which satisfy Equation (2.17), are known as the eigenvalues of $\mathbf{A}$. Equation (2.17) is referred to as the characteristic equation [1], [11].

After the linearization, the small-disturbance stability analysis may be performed using any of the methods applicable to linear systems. Generally, the modal analysis approach using eigenvalue techniques has many advantages [9]. Modal analysis approach using eigenvalue techniques gives a complete overview of the small-disturbance stability of the current system operating point, i.e. the equilibrium point about which the linearization is performed [10].

The following section lays the foundation for a discussion of the eigenvalue technique for small-disturbance angle stability analysis.

2.6 EIGENVALUES AND EIGENVECTORS IN STABILITY

2.6.1 Mathematical Definition

If $\mathbf{A}$ is considered to be the state matrix of dimension $(n \times n)$, the entries of $\mathbf{A}$ are real for a physical system like a power system [1]. Eigenvalues of the matrix $\mathbf{A}$ are given by the values of the scalar parameter λ for which there exist non-trivial solutions (i.e. solutions other than $\mathbf{\Phi} = 0$) to the Equation (2.18) below [1], [12]:

$$\mathbf{A\Phi} = \lambda\mathbf{\Phi} \tag{2.18}$$

where $\mathbf{\Phi}$ is an $n \times 1$ vector (i.e. column vector of length equal to the number of states).

The necessary condition that Equation (2.18) has non-trivial solutions is given by Equation (2.19) [1], [12].

$$\det(\mathbf{A} - \lambda\mathbf{I}) = 0 \tag{2.19}$$

The n solutions $\lambda = \lambda_1, \lambda_2, \ldots\lambda_n$ are referred to as eigenvalues of A.

The non-zero values of $\mathbf{\Phi}$ in (2.18) are referred to as the right eigenvectors corresponding to the eigenvalues. Similarly,

$$\mathbf{\Psi A} = \lambda \mathbf{\Psi} \tag{2.20}$$

where Ψ is the $1xn$ left eigenvector (row vector of length equal to the number of states) corresponding to the eigenvalue λ.

2.6.2 System Response, Eigenvalues and Eigenvectors

If $\mathbf{\Phi}_i$ and $\mathbf{\Psi}_i$ are considered the right and left eigenvectors of the state matrix $\mathbf{A}$, corresponding to the eigenvalue λ_i then:

$$\mathbf{A\Phi}_i = \lambda_i \mathbf{\Phi}_i \qquad i = 1,2,\ldots,n \tag{2.21}$$

$$\mathbf{\Psi}_i \mathbf{A} = \lambda_i \mathbf{\Psi}_i \qquad i = 1,2,\ldots,n \tag{2.22}$$

The right and the left eigenvectors corresponding to different eigenvalues are orthogonal. This means, if $\lambda_j \neq \lambda_i$ then, due to the orthogonal property of eigenvectors corresponding to different eigenvalues [1]:

$$\mathbf{\Psi}_j \mathbf{\Phi}_i = 0 \tag{2.23}$$

The orthogonal property of eigenvectors makes it possible for any vector of length n to be expanded in terms of eigenvectors. In the case of left and right eigenvectors corresponding to the same eigenvalue:

$$\mathbf{\Psi}_i \mathbf{\Phi}_i = C_i \tag{2.24}$$

where C_i is a non-zero constant. Since eigenvectors are only determined to within a scalar multiplier (i.e. $k\Phi_i$ is also a solution to (2.21) where k is a scalar), eigenvectors are usually normalized, such that [1]:

$$\mathbf{\Psi}_i \mathbf{\Phi}_i = 1 \tag{2.25}$$

If $\mathbf{R}$ is considered the matrix of n right eigenvectors given by:

$$\mathbf{R} = [\mathbf{\Phi}_1 \quad \mathbf{\Phi}_2 \quad \ldots \quad \mathbf{\Phi}_n] \tag{2.26}$$

and a matrix $\mathbf{L}$ of n linearly independent left eigenvectors i.e. n row vectors of length n transposed as given in the following equation:

$$L=[\ \Psi_1^T \quad \Psi_2^T \quad \ldots \quad \Psi_n^T\ ]^T \tag{2.27}$$

a diagonal matrix $\mathbf{M}$ with the eigenvalues $\lambda_1, \lambda_2, \ldots, \lambda_n$ as diagonal elements can be obtained as follows:

$$\mathbf{M} = \begin{bmatrix} \lambda_1 & & & \\ & \lambda_2 & & \\ & & \ddots & \\ & & & \lambda_n \end{bmatrix} \tag{2.28}$$

such that Equation (2.29) holds:

$$\mathbf{AR} = \mathbf{MR} \tag{2.29}$$

it follows from (2.29) that:

$$\mathbf{R}^{-1}\mathbf{AR} = \mathbf{M} \tag{2.30}$$

since

$$\mathbf{LR} = \mathbf{I}$$

then

$$\mathbf{L} = \mathbf{R}^{-1} \tag{2.31}$$

When the system is not in equilibrium, the system state variables change with time and the set of points traced by the system state in the state space as the system moves is called the state trajectory [1]. The stability of a linear system is independent of the input [1]. In order to study the zero input (free motion) time response of the linearized power system, consider the equation (system with zero input, $\mathbf{B} = 0$) [1]:

$$\Delta \dot{\mathbf{x}} = \mathbf{A}\Delta\mathbf{x} \tag{2.32}$$

Equation (2.32) has limitations in studying the free motion (motion of state trajectory, i.e. points traced out in the n dimensional space as the states change) of the system because, "*the rate of change of each state variable is a linear combination of all state variables and as a result of this cross-coupling between the states it is difficult to isolate those parameters that influence motion in a significant way*" [1].

In order to eliminate this cross-coupling, a new state vector $\mathbf{z}$ related to the original state vector by Equation (2.33) is introduced [1].

$$\Delta\mathbf{x} = \mathbf{R}\mathbf{z} \tag{2.33}$$

where $\mathbf{R}$ is the matrix of right eigenvectors of $\mathbf{A}$ defined by Equation (2.26). Substituting (2.33) into (2.32), gives [1]:

$$\mathbf{R}\dot{\mathbf{z}} = \mathbf{A}\mathbf{R}\mathbf{z} \tag{2.34}$$

The new state equation can then be written as [1]:

$$\dot{\mathbf{z}} = \mathbf{R}^{-1}\mathbf{A}\mathbf{R}\mathbf{z} \tag{2.35}$$

Substituting (2.30) into (2.35) gives:

$$\dot{\mathbf{z}} = \mathbf{M}\mathbf{z} \tag{2.36}$$

The transformation has uncoupled the new state equations. It is now evident in equation (2.36) that the orthogonality property of the left and right eigenvector enables the state equations to be uncoupled. Equation (2.36) represents n uncoupled first order equations [1]:

$$\dot{z}_i = \lambda_i z_i \tag{2.37}$$

where $i = 1,2,\ldots,n$

Equation (2.37) is a first order differential equation whose solution with respect to time is [1]:

$$z_i(t) = z_i(0)e^{\lambda_i t} \tag{2.38}$$

where $z_i(0)$ is the initial value of z_i.

The response in terms of the original state vector of Equation (2.32) is given by [1]:

$$\begin{aligned}\Delta\mathbf{x}(t) &= \mathbf{R}\mathbf{z}(t) \\ &= \begin{bmatrix}\boldsymbol{\Phi}_1 & \boldsymbol{\Phi}_2 & \cdots & \boldsymbol{\Phi}_n\end{bmatrix}\begin{bmatrix} z_1(t) \\ z_2(t) \\ \vdots \\ z_n(t)\end{bmatrix}\end{aligned} \tag{2.39}$$

which can be written in short substituting (2.38) into (2.39) giving [1]:

$$\Delta\mathbf{x}(t) = \sum_{i=1}^{n} \boldsymbol{\Phi}_i z_i(0)e^{\lambda_i t} \tag{2.40}$$

From Equation (2.39) it follows that [1]:

$$\mathbf{z}(t) = \mathbf{R}^{-1}\Delta\mathbf{x}(t) = \mathbf{L}\Delta\mathbf{x}(t) \tag{2.41}$$

which implies that [1]:

$$z_i(t) = \boldsymbol{\Psi}_i\Delta\mathbf{x}(t) \tag{2.42}$$

and for $t = 0$:

$$z_i(0) = \boldsymbol{\Psi}_i\Delta\mathbf{x}(0) \tag{2.43}$$

By using c_i to denote the scalar product $\boldsymbol{\Psi}_i\Delta\mathbf{x}(0)$, Equation (2.40) may be written as [1]:

$$\Delta\mathbf{x}(t) = \sum_{i=1}^{n} \boldsymbol{\Phi}_i c_i e^{\lambda_i t} \tag{2.44}$$

The response of the i^{th} state variable is given by:

$$\Delta x_i(t) = \boldsymbol{\Phi}_{i1}c_1e^{\lambda_1 t} + \boldsymbol{\Phi}_{i2}c_2e^{\lambda_2 t} + \cdots + \boldsymbol{\Phi}_{in}c_ne^{\lambda_n t} \tag{2.45}$$

Equation (2.45) means that the time domain response can be expressed as "*a linear combination of the n dynamic modes corresponding to the n eigenvalues of the state matrix* "[1]. In other words, the time domain response of each state variable depends on all the modes in the system. If a particular mode is excited, this will be visible in the time response of the state variable to a higher or lesser degree depending on the level of

activity of the mode in the state variable. Therefore, mode will refer to $\Phi_i c e^{\lambda_i t}$, e.g. Equation (2.45) and equation (2.44) is the modal decomposition of the solution $\Delta x(t)$. It should be noted that, "*the time dependent characteristic of a mode corresponding to an eigenvalue* λ_i *is given by* $e^{\lambda_i t}$" [1]. In [8] mode is defined as: "*the technical term for a specific oscillation pattern...It is used, more loosely, to refer to an oscillation at a specific frequency*".

2.6.3 Eigenvalues and Stability

The stability of the system is determined by the eigenvalues of the system in the following way [1]:

- A real eigenvalue corresponds to a non-oscillatory mode. A negative real eigenvalue corresponds to a decaying mode; the larger its magnitude, the faster the decay. A positive real eigenvalue represents an infinitely growing mode and this represents aperiodic instability. The values of the scalar constants c_i and eigenvectors Φ_i associated with real eigenvalues are also real thus making the entries of **x(t)** real.

- The matrix **A** is real, then complex eigenvalues always occur in conjugate pairs in the form given by [1]:

$$\lambda = \sigma \pm j\omega \tag{2.46}$$

"*Each conjugate pair corresponds to an oscillatory mode. The real part of the eigenvalues gives the damping, and the imaginary part gives the frequency of the oscillation. The frequency of oscillation in Hz is given by* [1]:

$$f = \frac{\omega}{2\pi} \tag{2.47}$$

The damping ratio is given by [1]:

$$\zeta = \frac{\sigma}{\sqrt{\sigma^2 + \omega^2}} \tag{2.48}$$

The damping ratio gives the rate of decay of the amplitude of the oscillation".

Figure 2.1 depicts the stable and the unstable regions of the complex plane of eigenvalues.

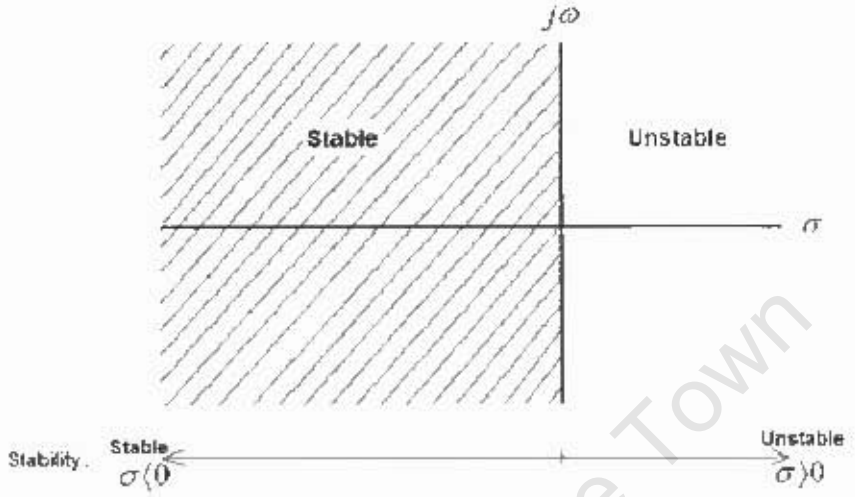

Figure 2.2: *The S-plane [adapted from 14]*

2.7 POWER SYSTEM OSCILLATIONS

2.7.1 Historical Review of Power System Oscillations

Power system oscillations are not new to the power system industry. In the beginning, generators were operating in isolation and the main stability problem at the time was the lack of synchronizing torque. Over time the demand for electricity has increased and the interconnection of generators was found to be a way to provide more power and increase the reliability of the power, system [8]. However, oscillations were experienced when generators were interconnected [8], although at that stage power system oscillations were not an issue for some time [1].

"At the time generators were fairly close to one another. Oscillations were at frequencies in the region of 1 to 2Hz were experienced" [1], [8]. It was discovered that this problem was due to insufficient damping. The problem was solved by the use of damper windings

in generator rotors and, turbine type prime movers with complimentary torque-speed characteristics [1], [8].

As the demand for power grew, generators started to operate close to their transient and small-disturbance stability limits.

"*In the 1950s and 1960s most of the industry's focus was on transient stability. Lack of synchronizing torque was the principal cause of instability in this era. High speed protection relays were developed. Fast acting high gain excitation systems were developed to prevent generators from losing synchronism following a fault.*"[8].

Whilst these trends improved transient stability, they increased the tendency of power systems to exhibit oscillatory instability [1], and so power system stabilizers were developed and tuned to damp these oscillations [8].

In the last few years, there have been many reported incidents of low frequency oscillations observed mostly on systems that are heavily loaded and interconnected via long transmission lines [20], [21]. "*In some incidents interconnections were put on hold until asynchronous HVDC interconnections were technically possible* "[8]. To this day, the characteristics and factors influencing low frequency oscillations are not very well understood [8] and a lot of research is being carried out around the world to tune power system stabilizers to damp oscillation over increased frequency ranges [16].

2.7.2 Types of Power System Oscillations

It has been mentioned previously that today the problem of small-disturbance stability is predominantly one of insufficient damping of oscillations, so it is worthwhile to gain insight into the different types of oscillations in power systems.

The following four different types of oscillations, classified according to interaction characteristics, have been experienced in power systems [1]:

- *Local plant modes*

"These oscillations are associated with one synchronous generator swinging against the rest of the power system, or electrically close synchronous generators swinging against each other. The term local arises from the fact that oscillations are localized at a small part of a power system." [1].

- **Inter-area modes**

"*These oscillations are associated with the swinging of groups of synchronous generators in one part of the power system swinging against groups of synchronous generators in other parts of the power system interconnected by a relatively weak transmission path or tie..*" [1].

- **Control Modes**

"*These oscillations are associated with generating units and other controls. Poorly tuned exciters, speed governors, HVDC converters and static var compensators are the usual causes of instability of the oscillations*" [1].

- **Torsional Modes**

"*These modes are associated with the turbine-generator shaft system rotational (mechanical) components. Instability of these modes may be caused by interaction with excitation control, speed governors, HVDC controls, and series-capacitor compensated lines*" [1].

CHAPTER 3
Overview of Various Analysis Techniques used in Small-disturbance Stability Analysis

3.1 INTRODUCTION

Small-disturbance stability analysis has a history of about a century or so [12]. This chapter gives a brief overview of the various techniques that have been employed for small-disturbance stability analysis in the past two decades, and then it moves on to discuss the powerful and currently widely used linear analysis technique, which is based on eigenvalues, sometimes referred to as modal analysis [8], [9], [12]. For the sake of simplicity, small-disturbance angle stability will simply be referred to as small-disturbance stability.

3.2 OVERVIEW OF VARIOUS ANALYSIS TECHNIQUES

There are many ways of analyzing the small-disturbance stability of a linearized power system; analytical techniques can be broadly divided into two categories, those in the frequency domain and those in the time domain [12]. However there are other methods used for small-disturbance analysis; these methods use static system characteristics and they are sometimes referred to as load flow methods and are only used for qualitative judgement to provide rough standards [12].

3.2.1 Time Domain Methods

There are two types of time domain methods, the numerical integration method, which includes the Runge-Kutta method, and the transit matrix method [12]. The numerical integration methods are extensively used in transient stability and are explained in detail in [1], [12]. In practice, small-disturbance stability analysis by this method is obtained by applying a minor disturbance such as opening a line for a very short time, about one cycle or less [12]. The disadvantage of the numerical integration method is that it takes longer than the eigenvalue method, but the advantage is that the waveforms of the various quantities can be obtained. Also, it enables non-linear effects to be added as necessary

[12].

3.2.2 Methods using System Static Characteristics

Among methods using system static characteristics is a method that determines the stability of the system using the phase differential angle, δ, which can be obtained from powerflow [12]. Another method determines the stability of the system using $\frac{\partial P}{\partial \delta}$, which can be derived from the power Jacobian matrix from powerflow [12].

3.3 MODAL ANALYSIS PERFORMANCE MEASURES

In the previous chapter, the relationship between eigenvalues and stability and the definition of eigenvalues and eigenvectors were discussed. This chapter moves on to discuss how eigenvalues and eigenvectors can be used to analyze the small-disturbance performance of a power system (i.e. how eigenvalues and eigenvectors can be used to analyse the small-disturbance stability).

3.3.1 Mode Shape and Eigenvectors

In the previous chapter, the response of the system in terms of the original state vector $\Delta\mathbf{x}$ and the transformed state vector $\mathbf{z}$ was discussed. Equation (2.39) and (2.41) in the previous chapter showed that $\Delta\mathbf{x}$ and $\mathbf{z}$ are related as follows:

$$\begin{aligned}\Delta\mathbf{x}(t) &= \mathbf{R}\mathbf{z}(t) \\ &= \begin{bmatrix}\boldsymbol{\Phi}_1 & \boldsymbol{\Phi}_2 & \dots & \boldsymbol{\Phi}_n\end{bmatrix}\begin{bmatrix} z_1(t) \\ z_2(t) \\ \vdots \\ z_n(t)\end{bmatrix}\end{aligned} \tag{3.1}$$

and

$$\begin{aligned}\mathbf{z}(t) &= \mathbf{R}^{-1}\Delta\mathbf{x}(t) = \mathbf{L}\Delta\mathbf{x}(t) \\ &= \begin{bmatrix}\boldsymbol{\Psi}_1^T & \boldsymbol{\Psi}_2^T & \dots & \boldsymbol{\Psi}_n^T\end{bmatrix}^T\begin{bmatrix} \Delta x_1(t) \\ \Delta x_2(t) \\ \vdots \\ \Delta x_n(t)\end{bmatrix}\end{aligned} \tag{3.2}$$

The original state vector $\Delta\mathbf{x}$ is a vector of original state variables chosen to represent the system dynamic performance and $\mathbf{z}$ is a vector of the transformed state variables such

that each variable is only associated with only one mode [1].

From Equation (3.1) it can be seen that the right eigenvector gives the relative activity of the state variables when a particular mode is excited, e.g. the relative activity of the state variable x_k in the i^{th} mode is given by the element Φ_{ki} of the right eigenvector $\mathbf{\Phi}_i$ [1], [8], [12]. The magnitudes of the elements of the right eigenvector $\mathbf{\Phi}_i$ give the relative activities of the n-state variables in the i^{th} mode, and the angles of the elements give phase displacements of the state variables with regard to the mode [1], [8], [12]. From Equation (3.2), it can be seen that: "*the left eigenvector $\mathbf{\Psi}_i$ identifies which combination of the original state variables displays only the i^{th} mode*" [1]. "*Thus the k^{th} element Φ_{ki} of the right eigenvector $\mathbf{\Phi}_i$ measures the activity of the k^{th} state variable x_k in the i^{th} mode, and the k^{th} element Ψ_{ki} of the left eigenvector $\mathbf{\Psi}_i$ weighs the contribution of this activity to the i^{th} mode*" [1], [8], [12].

3.3.2 Eigenvalue Sensitivity

Eigenvalue sensitivity discussed here is the sensitivity of eigenvalues to the change in the elements of the state matrix. Consider the equation which defines eigenvalues and eigenvectors [1]:

$$\mathbf{A}\mathbf{\Phi}_i = \lambda_i \mathbf{\Phi}_i \tag{3.3}$$

$\frac{\partial \lambda_i}{\partial a_{kj}}$ the sensitivity of the eigenvalue λ_i to the change in the element in the k^{th} row and j^{th} column a_{kj} of the state matrix $\mathbf{A}$ can be found by differentiating Equation (3.3) with respect to a_{kj} as follows [1]:

$$\frac{\partial \mathbf{A}}{\partial a_{kj}}\mathbf{\Phi}_i + \mathbf{A}\frac{\partial \mathbf{\Phi}_i}{\partial a_{kj}} = \frac{\partial \lambda_i}{\partial a_{kj}}\mathbf{\Phi}_i + \lambda_i \frac{\partial \mathbf{\Phi}_i}{\partial a_{kj}} \tag{3.4}$$

Pre-multiplying (3.4) by $\mathbf{\Psi}_i$, noting that right and left eigenvectors are scaled such that they are orthonormal (i.e. $\mathbf{\Psi}_i\mathbf{\Phi}_i = 1$) and $\mathbf{\Psi}_i(\mathbf{A} - \lambda_i\mathbf{I}) = 0$, Equation (3.4) simplifies to [1]:

$$\Psi_i \frac{\partial \mathbf{A}}{\partial a_{kj}} \Phi_i + \Psi_i (\mathbf{A} - \lambda_i \mathbf{I}) \frac{\partial \Phi_i}{\partial a_{kj}} = \frac{\partial \lambda_i}{\partial a_{kj}} \Psi_i \Phi_i$$
$$\Psi_i \frac{\partial \mathbf{A}}{\partial a_{kj}} \Phi_i = \frac{\partial \lambda_i}{\partial a_{kj}} \tag{3.5}$$

$\frac{\partial \mathbf{A}}{\partial a_{kj}}$ the rates of change of all elements of $\mathbf{A}$ with respect to the element a_{kj} are zero, except for the rate of change of a_{kj} with respect to a_{kj} which is 1, so Equation (3.5) can be further simplified to [1]:

$$\Psi_{ik} \Phi_{ji} = \frac{\partial \lambda_i}{\partial a_{kj}} \tag{3.6}$$

It can be seen then from Equation (3.6) that the sensitivity of the eigenvalue λ_i to a change in the element a_{kj} of the state matrix is equal to the product of the left eigenvector element Ψ_{ik} and the right eigenvector element Φ_{ji}.

Besides leading to the participation factors, which are discussed in the following section, eigenvalue sensitivity can provide useful information for studying measures for improving stability of a power system. However, this is not within the scope of this thesis and more information can be found in [12], [15].

3.3.3 Participation Factors

"*The problem in using left and right eigenvectors individually for identifying the relationship between the states and the modes is that the elements of the eigenvectors are dependent on units and scaling associated with state variables*" [1].

To solve this problem, a matrix called the participation matrix $\mathbf{P}$ which combines the right and left eigenvectors as a measure of the importance of a state to a mode was proposed in [16]. The columns of $\mathbf{P}$ are referred to as participation vectors and the elements of $\mathbf{P}$ are referred to as participation factors [16]. The participation matrix comprises of participation vectors $\mathbf{p}_i$ whose elements are participation factors as illustrated below [1]:

$$\mathbf{P} = \begin{bmatrix} \mathbf{p}_1 & \mathbf{p}_2 & \cdots & \mathbf{p}_n \end{bmatrix} \tag{3.7}$$

$$p_i = \begin{bmatrix} p_{1i} \\ p_{2i} \\ \vdots \\ p_{ni} \end{bmatrix} = \begin{bmatrix} \Phi_{1i}\Psi_{i1} \\ \Phi_{2i}\Psi_{i2} \\ \vdots \\ \Phi_{ni}\Psi_{im} \end{bmatrix} \tag{3.8}$$

Participation factors are defined by the element by element multiplication of the right and left eigenvectors as follows [12]:

$$p_{ki} = \Phi_{ki}\Psi_{ik} \tag{3.9}$$

and, p_{ki} measures the participation or the importance of the k^{th} state to the i^{th} mode. Participation factors are dimensionless because the left and right eigenvectors have reciprocal dimensions. Therefore; participation factors give an unbiased indication of the importance of a state to a mode [12].

3.3.4 Summary

Insufficient damping of power system oscillations is largely the problem in small-disturbance stability in power systems today [8]. Thus, the main aim of small-disturbance stability analysis is to examine if these oscillations die out so that the stability of the system is maintained [12].

Eigenvalues give information about the frequency and the damping of the mode. The real part of the eigenvalue gives the damping of the mode and the imaginary part gives the frequency of the oscillation.

Eigenvectors give the relationship between state variables and the mode. The right eigenvector component magnitudes indicate the relative activity of the state variables when a particular mode is excited. The angles of the right eigenvector components give the phase displacement of the state variables with regard to the mode. The phase separation of the right eigenvectors corresponding to the speed states of the generators assist in determining whether the generators are swinging together or not. When the generators are swinging together; they will have little or no phase separation and, when generators are swinging against each other, the phase separation will be large (about 180°). Whilst the right eigenvector measures the activity of a state variable in a mode, the left eigenvector weighs the contribution of this activity.

By studying the participation factor of the generator's speed state corresponding to a mode, the following important information can be obtained [8]:

- If the participation factor of the generator's speed state corresponding to a particular mode is real and positive, it implies that adding damping at that generator will increase the damping of the mode.

- If the participation factor of the generator's speed state corresponding to a particular mode is zero, it implies that adding damping at that generator will have no effect on the mode.

- If the participation factor of the generator's speed state corresponding to a particular mode is real and negative, it implies that adding damping at that generator will reduce the damping of the mode.

CHAPTER 4
Modelling of Power System Components for Stability Studies

4.1 INTRODUCTION

Power system planning and operating decisions rely on predictions of actual power system behaviour obtained from computer based simulation tools that employ mathematical models to represent the various physical components of the system [13]. It is therefore crucial that these mathematical models predict the behaviour of the actual power system as accurately as possible.

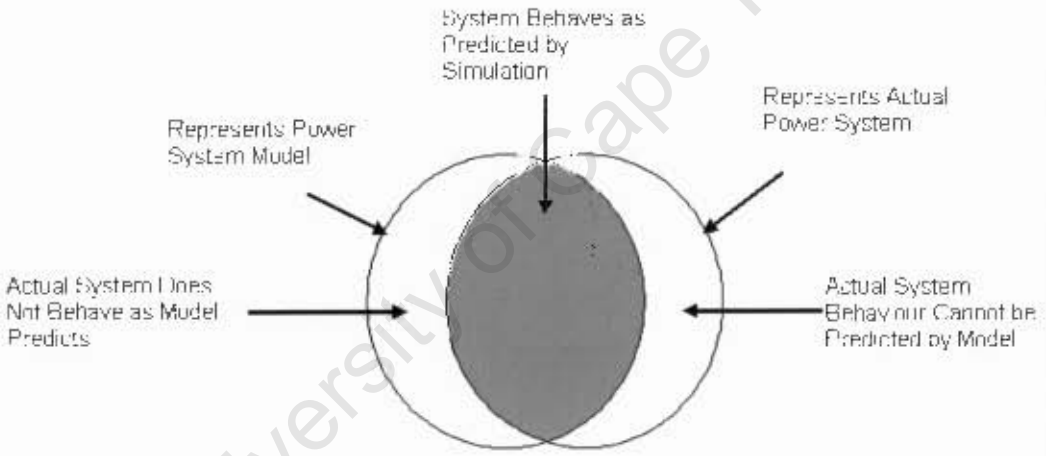

Figure 4.1: Concept of comparing system model behaviour to actual system behaviour [13]

The ideal in system modelling is to come up with a model that behaves exactly like the actual system. However, this is not possible in practice. Figure 4.1 illustrates the concept when comparing actual system behaviour with mathematical model behaviour [13]. It can be seen that there is the behaviour of the actual system that can be predicted by the mathematical model, the behaviour of the actual system that cannot be predicted by the model and the behaviour of the mathematical model that cannot be exhibited by the actual system. In an ideal situation, when the model behaves exactly the same as the actual system, the two circles completely overlap. The goal in system modelling is to

maximize the overlap between the two circles i.e. the model behaves almost like the actual system. The only reliable way to validate models is to do experiments and compare measured results with those obtained from the system model.

In this section, the recommended models for stability studies are discussed. Because of the wide scope of power system component modelling and time constraints for the purposes of this research, the discussion is restricted to the modelling of the synchronous generator, static loads, the simplified thyristor excitation system and the power system stabilizer (PSS).

4.2 SYNCHRONOUS GENERATOR MODELLING

The problem of small-disturbance angle stability is keeping interconnected synchronous machines in synchronism [1], [2], [11]. Therefore, it is crucial that the characteristics of synchronous machines are well understood and that the modelling of the dynamic behaviour of these machines is done as accurately as possible [1].

Synchronous generator modelling principles were developed in the 1920s [1], [22] and much progress has been made since then. The analysis of a synchronous generator is greatly simplified by Park's transformation, which projects the actual three-phase stator quantities onto a direct axis and a quadrature axis. The machine is represented by two coupled circuits, as shown in Figure 4.2 [24], whose parameters are time invariant, [22]. These parameters are obtained from tests and the manufacturer specifications of the synchronous generator. The simplest synchronous generator model used in stability analysis is the second order model, commonly known as the classical model. The model order ranges from second order to sixth order depending on the detail of the model. The mathematical equations included in each of the models can be found in [23]. The different order models are discussed below:

4.2.1 *Classical model* (second order model)

This is the simplest generator model in stability analysis. This model represents the generator by a constant voltage (E') behind a constant transient reactance (X_d'). It is generally used to represent synchronous generators in areas that are remote from the disturbance [22]. Two state variables are used by the classical machine model, the speed deviation $\Delta\omega$ and the rotor angle deviation $\Delta\delta$.

4.2.2 Third order model

The third order model improves the classical model by including the effects of a field circuit. The generator is represented by a variable voltage (E_q') behind a transient reactance (X_d'). Three state variables are needed by the third order model and the third state variable that is introduced in this model is the flux linkages in the field winding ψ_f. This model is generally used in salient pole machines, but it can also be used to represent simplified models of non-salient pole machines.

4.2.3 Fourth order model

The fourth order model extends the third order model by including the effects of electrical damping on the synchronous generator by adding a damper winding on the q-axis [23]. A fourth state variable introduced in this model is the flux linkages in the q-axis damper winding ψ_{1q}. The third and fourth order models are sometimes used in damping controller design where low order models are desired for computational efficiency.

4.2.4 Fifth order model

The fifth order model has been found to adequately represent the salient pole rotor synchronous generator in stability studies [11], [22], [24]. In this model, damper windings are included in the d- and q-axis. The electrical damping of the synchronous generator is modelled with these damper windings [23]. The fifth state variable introduced by the damper in the d-axis is the flux linkages in the d-axis damper winding ψ_{1d}.

4.2.5 Sixth order model

The sixth order model has been found to adequately represent the round rotor generator in stability studies [11], [23], [24]. The accuracy in modelling multiple paths for circulating eddy currents responsible for the electrical damping is improved when adding one extra damper winding on the q-axis [23]. In doing so, another state variable ψ_{2q}, which represents the flux linkages in the second q-axis damper winding, is introduced.

The synchronous generator model has been discussed considering the varying model details from the simplest second order model to the sixth order model. The sixth order model is the most detailed model available in PST. Figure 4.2 below depicts the d- and q-axis equivalent circuits of the sixth order model.

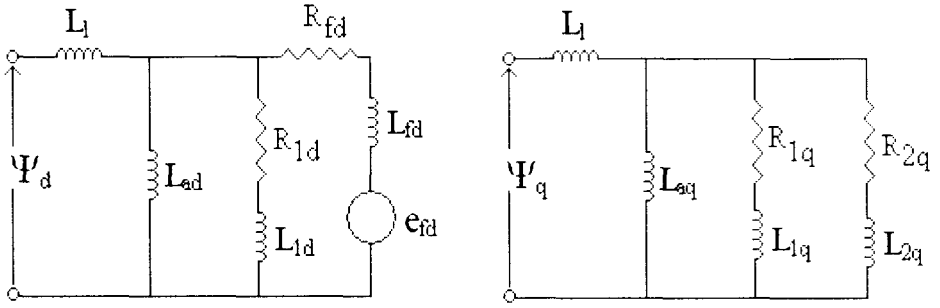

Figure 4.2: *The d-axis and q-axis equivalent circuits of the 6th order generator model [24]*

The sixth order model has six electrical circuits; it comprises the stator *d*- and *q*-axis circuits (L_l), the field circuit (R_{fd}, L_{fd}), one *d*-axis damper winding (R_{1d}, L_{1d}) and two *q*-axis damper windings (R_{1q}, L_{1q}, R_{2q}, L_{2q}). L_{ad} and L_{aq} represent the mutual inductance between the stator and the rotor circuits [24], [25].

4.3 MODELLING GENERATOR MAGNETIC SATURATION

There is no generally accepted method of representing generator saturation in small signal stability studies [13]. A number of different methods have been used to represent the effects of saturation in small signal stability studies [13], [22]. These include total saturation, incremental saturation and effective excitation [13].

Investigations on a single machine infinite bus carried out in [13] show that for the generator equipped with AVR without PSS, the damping ratio of the local modes obtained with saturation represented is higher than that with saturation neglected. Whith the generator equipped with AVR and PSS, "*the damping ratio obtained with incremental saturation and effective excitation methods is lower than that obtained with saturation neglected. However, for total saturation method, the damping ratio is not affected by saturation ...*"

Conclusions that can be drawn from these findings are that:

- The three saturation modelling methods have different effects on the local modes for different excitation control configuration
- For round rotor machines, both the d-axis and q-axis inductances are reduced when saturation is modelled.

Saturation is not very well understood but there is research going on in this field, [2], [13]. The effect of saturation on small-signal stability is beyond the scope of this thesis and thus is not considered in the case studies discussed.

4.4 MODELLING EXCITATION SYSTEMS AND POWER SYSTEM STABILIZERS

The primary function of an excitation system is to provide direct current to the field winding of the generator (rotor) [1]. The secondary function of the excitation system is the control of generator terminal voltage. It can also be used to assume protective functions (i.e., ensuring that the capability limits of the generator are not exceeded) [1]. The excitation control system can be divided into two components, the automatic voltage regulator (AVR) and the power system stabilizer (PSS) if present [1].

4.4.1 Exciters and AVR

Exciters have advanced from rotating dc exciters, through ac exciters with rotating rectifiers to static systems, which use thyristor bridges to generate the dc field voltage directly from the machine terminals [8]. The excitation system controls the generator terminal voltage.

The modelling of the simplified thyristor excitation system is the only excitation system discussed in this thesis. The discussion can be found in the subsequent chapters (5, 6 & 7). From experience and case studies conducted, it has been found that the effect of the fast acting, high gain AVR is to increase the synchronising torque and to decrease the damping torque [9]. This problem of reduced damping torque can be solved by connecting a PSS to the excitation control system.

4.5 POWER SYSTEM STABILIZERS

Power system stabilizers (PSS) are the most economical damping controls. A PSS is used to add a modulation signal to a generator's automatic voltage regulator reference input. In doing so, it produces an electrical torque on the generator proportional to speed deviation [8]. This provides additional damping torques on the shaft of the generator thereby improving the damping of power system oscillations. A typical power system stabilizer is made mainly from three building blocks [9]:

1. **Phase compensation:** these are the phase compensation circuits of the PSS. These circuits provide the phase lead to compensate for the phase lag between the exciter input and the electrical torque.
2. **Washout:** is a high pass filter that removes the dc offsets in the speed signal thereby eliminating the steady changes in speed so that, the stabilizer responds only to oscillations in speed.
3. **Gain:** the gain of the stabilizer determines the damping provided by the stabilizer.

4.6 MODELLING THE LOAD

Load modelling is important in power system stability. Load models are traditionally classified into two broad categories, static models and dynamic models [1].

"*A static load model expresses the characteristics of the load at any instant of time as algebraic functions of the bus voltage magnitude and frequency at that instant*" [1].

The response of most mixed loads (mix of dynamic and static loads) to reasonable amplitudes of voltage/frequency change is fast and the steady state of the response is reached very quickly [1], [3]. The use of static load models is acceptable in such instances. However, there are many cases where load dynamics have to be taken into consideration. Load models that take the dynamic characteristics of the load into consideration are known as dynamic load models. Examples of dynamic models are motors, water heaters, voltage controlled capacitor banks etc. [1].

In this research, the discussion of load modelling is restricted to static load models. The traditional method of modelling static loads is [1]:

$$P = P_0\left(\frac{V}{V_0}\right)^a \tag{4.1}$$

$$Q = Q_0\left(\frac{V}{V_0}\right)^b \tag{4.2}$$

where P and Q are the active power component and reactive power component when the bus voltage is V [1]. The subscript $_0$ indicates the values of the respective variables at the initial operating condition. Parameters of this model are a and b for the real and reactive power respectively. When these exponents are equal to 0, 1 and 2, the model represents a

constant power, a constant current or a constant impedance characteristic, respectively [1].

Another model used to represent static loads is the polynomial model commonly referred to as the ZIP model [1]:

$$P = P_0[p_1\overline{V}^2 + p_2\overline{V} + p_3] \tag{4.3}$$

$$Q = Q_0[q_1\overline{V}^2 + q_2\overline{V} + q_3] \tag{4.4}$$

where $\overline{V} = \frac{V}{V_0}$

The advantage of using this model is that the load can have one, two or all three characteristics (constant impedance, constant current and constant power). The parameters are p_1 to p_3 and q_1 to q_3 which define the portion of the constant impedance, constant current and constant power characteristic respectively [1]. Since each of these parameters represents a fraction / percentage of the total, p_1, p_2 and p_3 must always add up to unity. Similarly q_1, q_2, q_3 must add up to unity.

CHAPTER 5
Capabilities of PST for Small-Disturbance Stability Analysis

5.1 INTRODUCTION

PST is a collection of MATLAB files and these files enable the user to perform power system simulations [27], [28]. PST was first developed by Joe Chow of Rensselaer Polytechnic Institute and later marketed and improved by Cherry Tree Scientific Software [26], [30].

This chapter discusses the capabilities of PST for small-disturbance stability analysis. Section 5.2 gives an overview of what PST is. Section 5.3 discusses the modelling capabilities of PST. Section 5.4 discusses the linearization of the dynamic system equations and the eigenvalue calculation in PST. Lastly, Section 5.5 closes the chapter by discussing the special or useful features of PST.

5.2 OVERVIEW OF POWER SYSTEM TOOLBOX

PST is capable of performing load flow, small-disturbance and transient stability simulations. When performing a small-disturbance stability simulation in PST the first step is to input the system data. PST then performs a load flow simulation to calculate the system operating parameters ("system operating point"). From the load flow solution the dynamic models used in the small-disturbance simulation are initialized. The small-disturbance simulation is performed and the linearized system is calculated.

5.3 THE MODELLING CAPABILITIES OF PST

Dynamic models in PST are coded as MATLAB functions [27]. Power system component models in PST include [27]:

5.3.1 Generator models

- Classical model referred to as the electromechanical model in PST.
- Fourth order model referred to as the transient model in PST.
- Sixth order model referred to as the subtransient model in PST.

- Infinite bus is modelled as a classical generator model
- Excitation system models
- Simplified exciter model
- IEEE type DC1 and DC2.
- IEEE type ST3.
- Power system stabilizer model
- Simplified turbine governor model
- Induction motor model
- Induction generator model
- Static VAR compensator model
- Load modulation control
- HVDC line model
- Non-conforming load model
- Line flow function
- Utility functions
- Power system stabilizer design
- Frequency response from state space
- Step response from state space system models

Because of the wide scope of power system components modelling and the time constraints, the component models discussed in this thesis are those used in the test systems presented in chapter 8.

5.3.2 Generator Models in PST

The different order generator models are characterised by different states. Table 5.1 below shows the states present in the different order generator models.

Table 5.1: Table of the generator states characterizing the different order models in PST

State	Classical Model (2 states)	4th Order Model (4 states)	6th Order Model (6 states)
$\Delta\delta$	1	1	1
$\Delta\omega$	1	1	1
$\Delta E'_q$	-	1	1
$\Delta E'_d$	-	1	1
$\Delta\psi''_d$	-	-	1
$\Delta\psi''_q$	-	-	1

A "1" indicates that a state is modelled and a "-" if not.

In the above Table, $\Delta E'_q$, $\Delta E'_d$, $\Delta\psi''_d$ and $\Delta\psi''_q$ represent the voltage proportional to the field flux linkage, voltage proportional to the q-axis amortisseur flux linkage, d-axis amortisseur flux linkage and q-axis amortisseur flux linkage respectively.

5.3.3 Classical model

The classical model represents the synchronous generator as a constant voltage behind a transient reactance. The classical model is characterized by two states, the speed deviation $\Delta\omega$ and angle deviation $\Delta\delta$ (See table 5.1).

5.3.4 Fourth order model

The fourth order model extends the classical model by including the effects of the field winding and one damper winding on the q-axis. The fourth order model is sometimes used in damping controller design, where controller design algorithms are simpler with low order generator models. This model is characterized by four states as shown in table 5.1. In this thesis, the fourth order model will not be discussed further since, it was not used in any of the case studies carried out.

5.3.5 Sixth order model

The sixth order model extends the classical model by including the effects of the field winding, the damper windings, one damper winding on the d-axis and two damper windings on the q-axis. The second damper winding on the q-axis improves the accuracy of modelling multiple paths for circulating eddy currents [23]. This model is the

recommended model for representing round rotor generators in stability studies [22]. In PST, there is a limitation on the sixth order model in that it is assumed $X_d'' = X_q''$ even if $X_d'' \neq X_q''$.

5.3.6 Generator Magnetic Saturation Representation

In PST, it is assumed that both the d-axis and the q-axis have similar saturation characteristics. Whilst this assumption is not strictly correct, it has little effect on the accuracy of the saturation model [13]. In PST, it is assumed that there is no saturation for a field current less than 0.8pu. The user specifies two saturation coefficients, S(1.0) and S(1.2), corresponding to the 1.0 and 1.2pu terminal voltage (flux linkage), respectively [27]. These saturation parameters are determined from the open circuit saturation curve of the generator [1], [24], [25], [27]. The generator open circuit characteristic in PST is shown below in Figure 5.1.

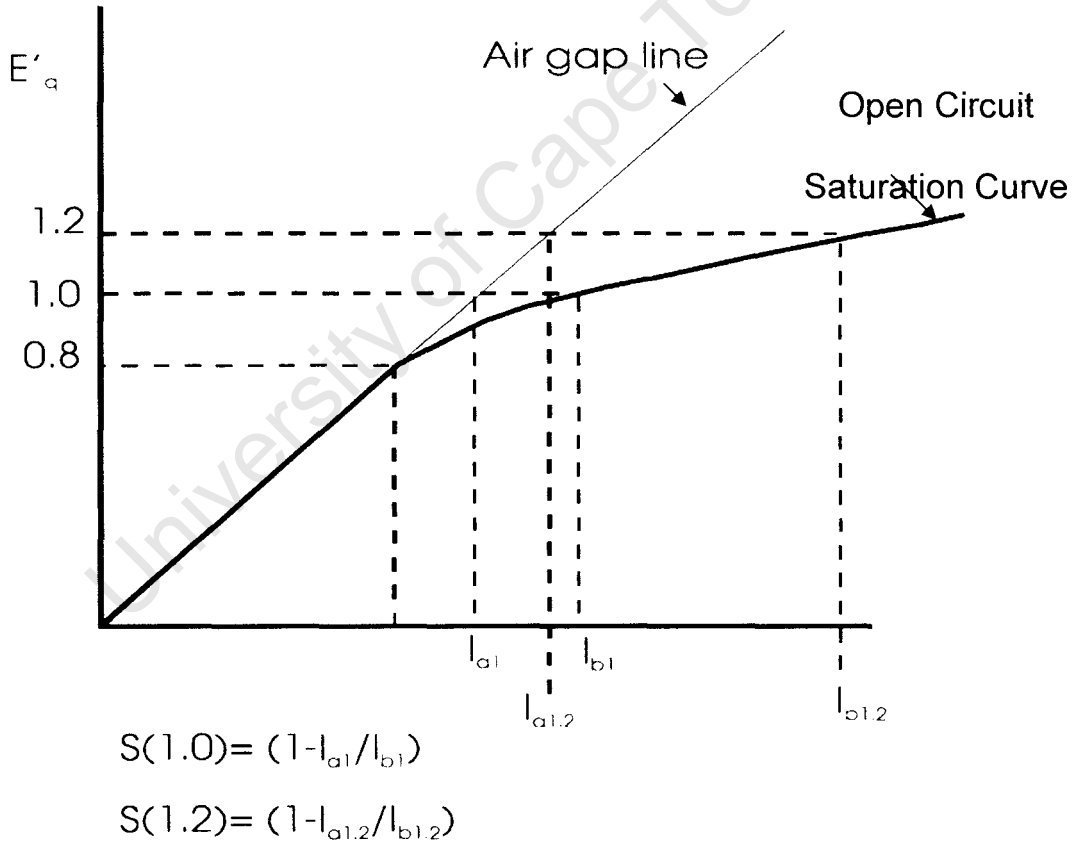

Figure 5.1: *Generator open circuit saturation characteristic [27]*

In figure 5.1, I_{a1} and $I_{b1}$are the field currents corresponding to 1.0 pu terminal voltage on

the air gap line and the open circuit saturation curve, respectively.

$I_{a1.2}$ and $I_{b1.2}$ are the field currents corresponding to 1.2 pu terminal voltage on the air gap line and the open circuit saturation curve, respectively.

5.3.7 Excitation System Models

There are four excitation system models available in PST. These are:

- the simplified exciter model
- IEEE type DC1
- IEEE type DC2
- IEEE type ST3 [27].

The simplified exciter model is the excitation system employed in the two test systems studied. This will be the only excitation system model that will be discussed in detail. The simplified exciter model is used to represent the simple thyristor exciter with AVR used on the single machine infinite bus and the four-generator two-area system. The simplified exciter model block diagram is shown below in Figure 5.2. Figure 5.2 shows two blocks, the transient gain reduction block and the AVR block. The transient gain reduction block is not used anywhere in the case studies conducted.

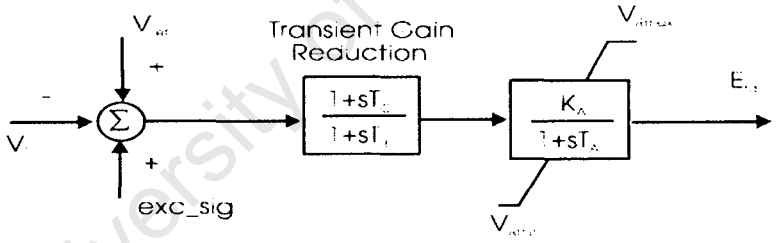

Figure 5.2: *The simplified exciter model in PST [27]*

5.3.8 Power System Stabilizer Model

The power system stabilizer model in PST has an option of a speed or power input, a washout filter and a lead-lag block. The block diagram of the power system stabilizer model in PST is shown in Figure 5.3.

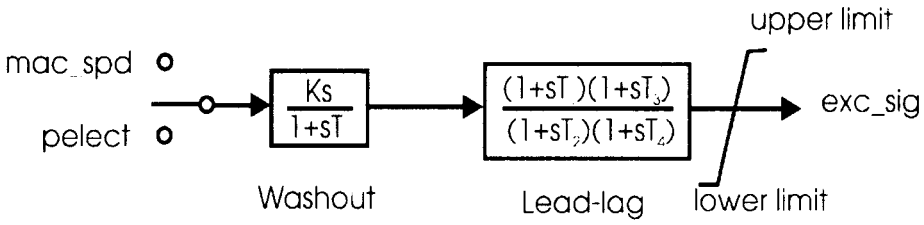

Figure 5.3: *Power system stabilizer model in PST [27]*

5.3.9 Modelling the Load

The discussion is restricted to the modelling of static loads. In PST, it is possible to model the load as constant impedance, constant current, constant power or a combination of the three [27]. This means that PST uses the polynomial type load modelling discussed in Section 4.5. In the two-area four-generator test system from [1], the active components of loads have constant current characteristics and the reactive components have constant impedance characteristics.

5.3.10 Transmission Line Representation

The pi-model is used for transmission line representation. The pi-model uses an equivalent pi-circuit to represent the transmission line. Figure 5.4 depicts the equivalent pi-circuit and, I_s is the sending end current, I_r is the receiving end current, V_s is the sending end voltage, V_r is the receiving end voltage, Z is the transmission line impedance and $B/2$ is the shunt susceptance. The pi-model model is the most widely used method for transmission line representation [12].

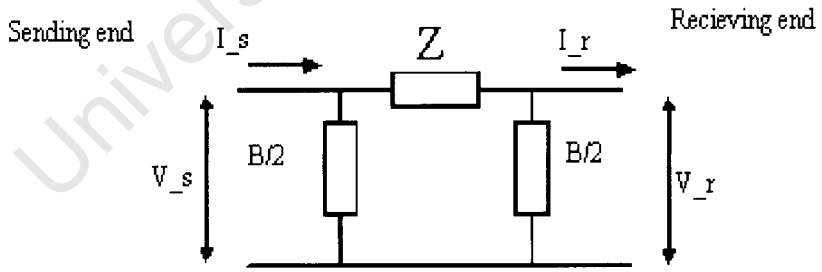

Figure 5.4: *Equivalent pi-circuit of a transmission line*

5.3.11 Infinite Bus Representation

The infinite bus is modelled using the classical model. In PST, the user indicates if a machine is to be modelled as an infinite bus. Since the infinite bus usually represents the external network or a relatively large system, the MVA rating of the infinite bus must

reflect this by having a significantly higher MVA rating than the generator (According to [28], the MVA of the infinite bus can be set to 80–100 times that of the generator).

5.4 LINEARIZATION IN PST

5.4.1 Introduction to Linearization in PST

In order to perform small-disturbance stability analysis, the nonlinear system dynamic equations are linearized about an operating point set by the load flow to get a linear set of Equations (2.12) and (2.13) as discussed in chapter 2 (and repeated below):

$$\Delta \dot{\mathbf{x}} = \mathbf{A}\Delta\mathbf{x} + \mathbf{B}\Delta\mathbf{u}$$
$$\Delta\mathbf{y} = \mathbf{C}\Delta\mathbf{x} + \mathbf{D}\Delta\mathbf{u}$$

In other small-disturbance stability analysis tools available in the market, such as MatNetEig, the state matrices $\mathbf{A}$, $\mathbf{B}$, $\mathbf{C}$ and $\mathbf{D}$ are calculated analytically from the Jacobians of the nonlinear state equations, whereas in PST the linearization (calculation of state matrices) is performed numerically [27].

5.4.2 The Linearization Process

The linearization process in PST is as follows [27]:

- Starting from the states determined from model initialization, a small perturbation Δx_i is applied to each state i in turn and $i = 1,2,3,\ldots,n$ where n is the total number of states
- For each state disturbed, the change in the rates of change $\Delta \dot{\mathbf{x}}$ of all state variables is calculated.
- $\Delta \dot{\mathbf{x}}$ is then divided by the perturbation applied to the i^{th} state Δx_i giving $\frac{\Delta \dot{\mathbf{x}}}{\Delta x_i}$, which is the column of $\mathbf{A}$ corresponding to the i^{th} state.

A matrix referred to as the permutation matrix is used to arrange states in a logical fashion. Following the calculation of $\Delta \dot{\mathbf{x}}$, the perturbed state is returned to its equilibrium value and the intermediate (transitional) variable values are reset to their initial values. This process is done for all the state variables calculating all the columns of $\mathbf{A}$. The other state matrices $\mathbf{B}$, $\mathbf{C}$ and $\mathbf{D}$ are calculated in a similar manner [27].

5.4.3 Calculation of Eigenvalues

The eigenvalues of the state matrix **A** are calculated using the MATLAB **eig** function, which uses the QR method and it calculates all the eigenvalues of **A**. Because PST uses the MATLAB **eig** function, which performs a full modal analysis on **A** (calculates all eigenvalues of **A**) and because of storage considerations, PST can only handle systems of up to 200 states [27].

5.5 SPECIAL FEATURES OF PST

Apart from the calculation of eigenvalues and their associated left and right eigenvectors, which are reasonably standard for small-disturbance analysis packages, PST has the following features:

- A matrix of participation factors is calculated and stored in a matrix called **p**
- A matrix of normalized participation factors greater than 0.1 is calculated and stored in a matrix called **p_norm**
- The normalized participation factors associated with rotor angles are stored in a matrix called **pr**. These are the participation factors of speed states of generators in the modes
- The damping ratios of the modes are calculated and stored in a matrix called **damp**
- The frequencies of the modes are calculated and stored in a matrix called **freq**
- It is possible for the user to view all state variables associated with a generator and its controls. It is also possible to view state variables associated with other dynamic devices in the system, if any
- The user can view the:
    - plot on the complex plane of all eigenvalues with damping ratio less than 0.05
    - plot on the complex plane of all eigenvalues with damping ratio greater than 0.05
    - plot of magnitudes of participation factors associated with unstable modes
    - plot of magnitudes of participation factors associated with modes having a damping ratio less than 0.05
    - plot of magnitudes of participation factors associated with rotor angle

modes

- It is possible for the user to perform a step and frequency response of a power system. The step response is a time domain simulation of the response of a system to a small "step" disturbance.

CHAPTER 6
Capabilities of MatNetEig for Small-Disturbance Stability Analysis

6.1 INTRODUCTION

MatNetEig is a power system analysis toolbox for small-disturbance stability analysis that is developed by the same company, Cherry Tree Scientific Software, that developed Power System Toolbox (PST) [32]. Unlike PST, MatNetEig cannot carry out transient stability simulations. MatNetEig interfaces with MatNetFlow, which is a toolbox for performing load flow [33]. MatNetFlow comes with the MatNetEig package.

This chapter discusses the capabilities of MatNetEig for small-disturbance stability analysis. Section 6.2 gives an overview of MatNetEig. Section 6.3 discusses the modelling capabilities of MatNetEig. Section 6.4 discusses the linearization of the dynamic system equations and the eigenvalue calculation in MatNetEig. Lastly, Section 6.5 closes the chapter by discussing the special or useful features of MatNetEig. Because there are many similarities between PST and MatNetEig the differences will mostly be highlighted in this chapter.

6.2 OVERVIEW OF MATNETEIG

Unlike PST, MatNetEig can handle bigger systems. MatNetEig can perform modal analysis (calculate all eigenvalues) on systems having up to 1000 states and not 200 like PST. Like PST, MatNetEig uses the QR method to calculate eigenvalues [12], [27], [29], [36]. The difference lies in the approach used. The tools that can handle bigger systems use the sparsity property of the state matrix to calculate a selection of eigenvalues [27], [36]. Like in PST, in MatNetEig data is input in matrices. Files are written in the format of PST. With MatNetEig it is also possible to use a graphical user interface when executing the input data unlike in PST, where the user always has to type commands on the MATLAB command window.

6.3 MODELLING CAPABILITIES OF MATNETEIG

Dynamic models in MatNetEig are programmed as MATLAB functions but internally the data is handled differently from the way it is in PST since MatNetEig is an object-oriented program and PST is not [32]. According to [32], MatNetEig can model the following power system elements:

- Generator models
- Classical model
- Sixth and fifth order model (called Subtransient in the software documentation) for round rotor and salient pole rotor generators respectively.
- Saturation is modelled on each axis in both models, in the round rotor model, the saturation of the d- and q- axis are coupled and, in the salient pole model the saturation in the two axis are decoupled
- Infinite bus is modelled as a classical generator model and the infinite bus states are removed by a special command
- Excitation system models
- All standard IEEE exciter models
- Governor Systems
- Thermal and hydraulic turbine governor models
- Induction Machines
- Induction motors and induction generators
- FACTS
- Static VAR Compensator
- Thyristor Controlled Series Compensator
- Unified Power Flow Controller
- Active load modulation
- Reactive load modulation
- Power system stabilizer model.
- Transmission line model is the pi-model.

As mentioned before in the previous chapter, because of the wide scope of power system

components modelling and the time constraints, the component models discussed in this thesis are those found on the system models used as test systems presented in chapter 8.

6.3.1 Generator Models in MatNetEig

The improvement of MatNetEig over PST is that the limitation in PST that $X_d'' = X_q''$ no longer exists. In MatNetEig X_d'' and X_q'' can have different values. As for the rest, the generator modelling in MatNetEig is very similar to that of PST. See the previous chapter Section 5.3.

6.3.2 Generator Magnetic Saturation Representation in MatNetEig

In MatNetEig magnetic saturation is modelled by varying the magnetizing reactances X_{ad} and X_{aq} as a function of the airgap flux linkage ψ_a [34]. The open circuit characteristic function is defined by the saturation coefficients S1 and S2, and type of saturation curve or saturation type. See Figure 6.1 obtained from [34].

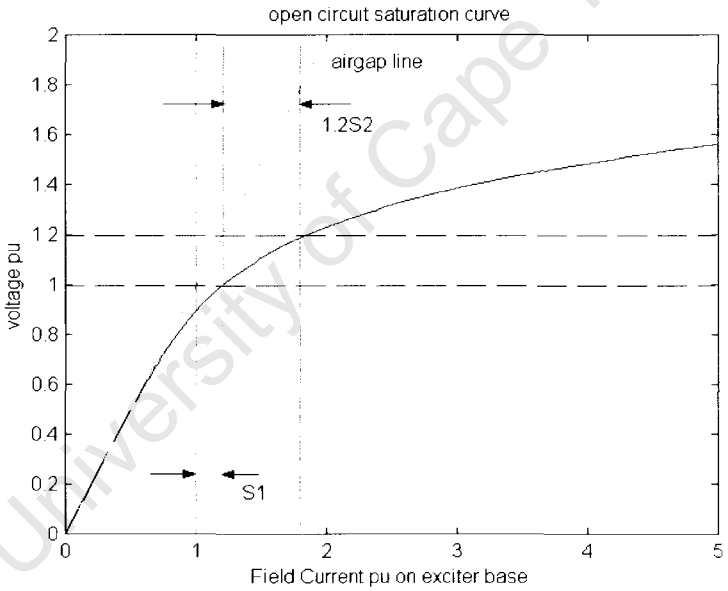

Figure 6.1: *Open circuit saturation characteristics [34]*

There are three saturation types defined in MatNetEig. The excitation current varies the airgap flux linkage ψ_a in three ways. In MatNetEig, the saturation type chosen is influenced by the generator type. The following are the three different types of saturation modelling in MatNetEig [34]:

Saturation Type 1

$$b_{sat} = 5.0\log(\frac{1.2S_2}{S_1}) \tag{6.1}$$

$$a_{sat} = S_1 e^{-0.2*b_{sat}} \tag{6.2}$$

$$i = \psi_a + a_{sat} e^{b_{sat}(\psi_a - 0.8)} - a_{sat} \tag{6.3}$$

Saturation Type 2

$$i = \psi_a + a_{sat}(\psi_a - b_{sat})^2 \tag{6.4}$$

$$\psi_a > b_{sat} \tag{6.5}$$

$$k1 = (1.2S_2 - S_1)$$
$$k2 = 2.4(S_2 - S_1)$$
$$k3 = (1.2S_2 - 1.44S_1)$$
$$b_{sat} = \frac{(k2 - \sqrt{(k2)^2 - (4*k1*k3)})}{(2*k1)}$$
$$a_{sat} = \frac{1.2S_2}{(1.2 - b_{sat})^2} \tag{6.6}$$

Saturation Type 3

$$i = \psi_a + a_{sat}(\psi_a)^{b_{sat}} \tag{6.7}$$

$$a_{sat} = S_1 \tag{6.8}$$

$$b_{sat} = \frac{\log(\frac{1.2S_2}{S_1})}{\log(1.2)} \tag{6.9}$$

6.3.3 Excitation System Models

All the standard IEEE models are available in MatNetEig. The IEEE AC4A exciter will be discussed here, as it was the model used in the case studies conducted. The IEEE AC4A was used to model a simple thyristor exciter with AVR. The block diagram of the excitation system is shown below in Figure 6.2 from [35]. The first block in Fig. 6.2 was not used in the case studies conducted. For the second block, K_a and T_a are the exciter gain and exciter time constant, respectively. This system is very similar to that in PST

(See also Figure 5.2 in the previous chapter).

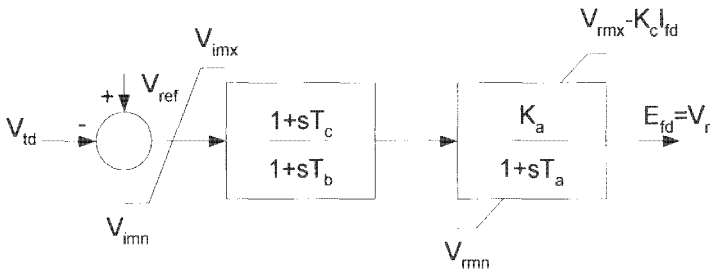

Figure 6.2: *IEEE AC4a excitation system [35]*

6.3.4 Power System Stabilizer Model

The stabilizer model is similar to that in PST and the block diagram is shown below in Figure 6.3, and it is taken from [35]. As in PST, it has an option of a speed or power input. The input is indicated as u in the figure (See also Figure 5.3 in the previous chapter).

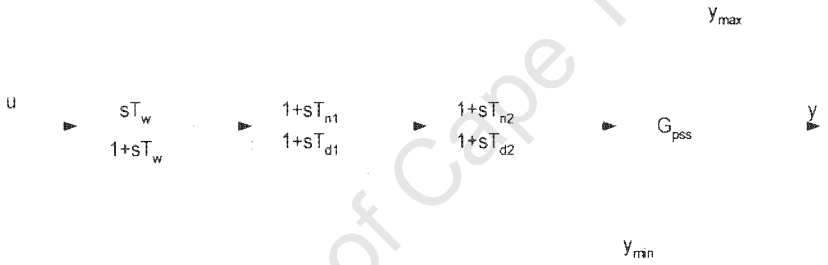

Figure 6.3: *Power system stabilizer model in MatNetEig [35]*

6.3.5 Transmission Line Representation

Like in PST, the pi-model is used as discussed in Section 5.3.6.

6.3.6 Load Modelling

Like in PST, the loads in the case studies conducted are static loads. Load is modelled in the same way as in PST, as discussed in Section 5.3.5.

6.3.7 Infinite Bus Representation

The infinite bus representation is represented in the same way as in PST, using a classical generator model as discussed in Section 5.3.7.

6.4 LINEARIZATION IN MATNETEIG

6.4.1 The Linearization Process

Linearization in MatNetEig is analytical and not numerical like in PST. Numerical linearization was discussed in the previous chapter and, analytical linearization was discussed in chapter 2.

6.4.2 Calculation of Eigenvalues

MatNetEig forms a sparse set of linear differential/algebraic equations for the power system [36]. The full state space equations are formed from this sparse model by eliminating the network algebraic variables [36]. Performing full modal analysis in MatNetEig limits system size of the systems that can be handled (about 200 states) [32], [36]. Partial modal analysis may be performed on very large system (systems of over 1000 states) [32], [36].

6.5 SPECIAL FEATURES OF MATNETEIG

Apart from the calculation of eigenvalues and their associated left and right eigenvectors, which are reasonably standard for small-disturbance analysis packages, MatNetEig has the following features [36]:

- A matrix of participation factors is calculated and stored in **p**
- A matrix of normalized participation factors greater than 0.1 is calculated and stored in **p_norm**
- The damping ratios of the modes are calculated and stored in **damp**
- The frequencies of the modes are calculated and stored in **freq**
- It is possible for the user to view all state variables associated with a generator and its controls. It is also possible to view state variables associated with other dynamic devices in the system if any
- The user can make use of the graphical user interface invoked by typing *ssview* in the command window. The GUI adds no new functions but, makes it faster to access the different variables by clicking on them.

It is possible for the user to perform a step and frequency response of a power system. The step response is a time domain simulation of the response of a system to a small "step" disturbance.

CHAPTER 7
Capabilities of CPAT S-Method for Small Signal Stability Analysis

7.1 INTRODUCTION

The CRIEPI Power System Analysis Tool (CPAT) was developed sometime before 1980 to assess bulk power systems [37]. CREIPI is the Central Research Institute of Electric Power Industry [37]. CPAT comprises three modules; there is the L-Method, the Y-Method and the S-Method, which are for running power flow, nonlinear transient stability and small-disturbance stability simulations respectively [37].

This chapter discusses the capabilities of the CRIEPI Power System Analytical Tool (CPAT) for small-disturbance stability analysis. Section 7.2 gives an overview of CPAT. Section 7.3 discusses the modelling capabilities of CPAT. Section 7.4 discusses the linearization of the dynamic system equations and the eigenvalue calculation in CPAT. Lastly, Section 7.5 closes the chapter by discussing the special or useful features of CPAT.

7.2 OVERVIEW OF CPAT

Unlike the other two simulation tools that run on MATLAB, CPAT runs on a different platform called POPONAS [38]. POPONAS is a dialog-driven man-machine interface program developed by the Denryoku Computing Center [38]. CPAT uses the S-method, which takes a different approach from MatNetEig and PST to calculate eigenvalues.

CPAT can handle systems with up to 1500 buses, 300 generators and 1800 branches. This means for generators modelled by 10 differential equations, the system can handle up to 3000 states.

7.2.1 The L-Method

The L-Method is the module of CPAT that performs load flow calculations. To do load flow calculations the L-Method employs the well-known Newton Raphson method [12]. More information on the Newton Raphson method can be found in [1], [12].

7.2.2 The S-Method

The S-Method is the module of CPAT that performs small-disturbance stability calculations. The S-Method calculates eigenvalues and eigenvectors associated with poorly damped modes [12].

7.2.3 The Y-Method

The Y-Method is that module of CPAT that performs transient stability calculations. Using this method the user can simulate events like faults on the system. Since the focus of this research is on small-disturbance stability, only the S-Method will be discussed in detail. For more information regarding the Y-Method, see [12], [37].

7.3 MODELLING CAPABILITIES OF CPAT

With components modelling, CPAT is the most flexible of the three since it allows the user to use special blocks to design generator controls (excitation system, PSS, governor) [37]. Special blocks are the different building blocks a user needs to design generator controls. Examples of special block elements include gain blocks, lead-lag blocks, integrators, etc.

Power system component models in CPAT include [37]:

- Generator models
- Generator model order varies from classical 2^{nd} order up to the 6^{th} order. There is the 2^{nd}, 3^{rd}, 4^{th}, 5^{th}, and 6^{th} order model
- Infinite bus is modelled as a classical generator model
- Excitation system models
- There are eleven types available to the user
- The user can build a custom excitation system model using special blocks
- Power system stabilizer model
- There are three stabilizer input options available to the user: power input, speed input or frequency input
- The user can use special blocks to construct a custom based PSS
- Governor Systems
- Two types of hydroelectric turbine governors
- Eleven types of thermal turbine governors

- One type of nuclear turbine governor
- Transmission line models
- T-type equivalent circuit model
- Pi-type equivalent circuit model (used in the case studies conducted)
- Distributed parameters model
- Load Models
- Static loads
- Dynamic loads

As mentioned in the previous chapter, because of the wide scope of power system components modelling and the time constraints, the component models discussed in this thesis are those found on the system models used as test systems presented in chapter 8.

7.3.1 Generator Models

In generator modelling, CPAT is the most flexible in terms of the different order models available to the user. The user can choose any model order for the generator ranging from the classical model (second order model) up to the very detailed sixth order model. The different order generator models have been discussed in detail in Chapter 4.

7.3.2 Generator Magnetic Saturation Modelling in CPAT

CPAT outperforms the other packages in the modelling of saturation, in that it allows for different d- and q-axis open circuit saturation characteristics. To model the saturation, the user is required to enter the point SY(1) where saturation starts, the point corresponding to 1.0 pu terminal voltage and a minimum of one point on the nonlinear saturation characteristic. Up to nine points can be entered to improve the accuracy of the curve modelling the nonlinear characteristic. See Figure 7.1 below.

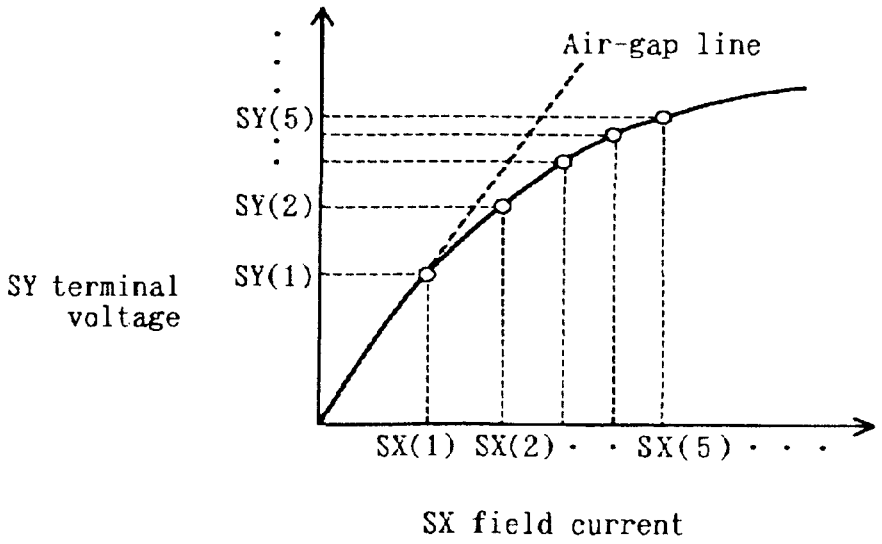

Figure 7.1: *Open circuit saturation characteristic in CPAT [37].*

Whilst the package allows for different saturation characteristics for the d-axis and the q-axis, it is generally difficult to obtain a saturation curve on the q-axis [12]. Usually the value used for the synchronous reactance of the q-axis is made smaller than that for the synchronous reactance of the d-axis (unsaturated value), so that saturation can be considered equivalently [12]. However, if the saturation characteristic of the q-axis is known, it is recommended in [12] that this characteristic can also be considered.

7.3.3 Excitation System Model

There are eleven kinds of programmed/built-up (ready to use) excitation systems [37]. With special blocks, the user can build customized excitation systems [37], which makes CPAT very flexible when it comes to modelling generator controls.

For the case studies conducted in this thesis, the excitation system simulated was built using special blocks to obtain the simplified exciter model. The block diagram of the excitation system (e.g., AVR and PSS) is shown in Figure 7.2.

7.3.4 PSS Model

There are four kinds of programmed/built-up (ready to use) power system stabilizer models [37]. With special blocks, the user can build custom power system stabilizer models [37]. For the input to the PSS, the user has a choice between generator active power, generator rotor speed deviation and bus frequency deviation [37].

For the case studies conducted in this thesis, the PSS simulated was built using special blocks to match the PSS that is used in the test system models (presented in chapter 8). Special blocks allow the user to build an excitation system control model as if the user were preparing a block diagram of the excitation system. Special blocks comprises of various building elements like, gain blocks, lead-lag blocks, summers, limiters etc. Using these building elements the user can build custom excitation system control models. The block diagram of the PSS simulated connected to the exciter is shown in Figure 7.2.

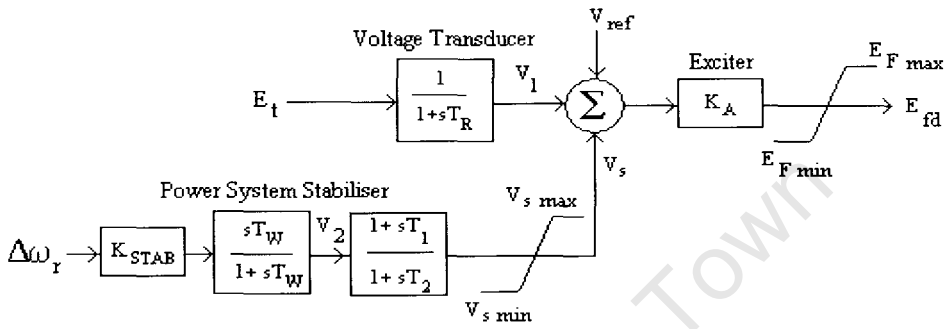

Figure 7.2: *PSS connected to the exciter [1].*

7.3.5 Transmission Line Models

The user has a choice of transmission line models. These models include the pi-type equivalent circuit model and the T-type equivalent circuit model [12], [37].

For the case studies conducted in this thesis, the pi-model is used to model the transmission line. The pi-type equivalent circuit model was discussed in chapter 5.

7.3.6 Load Models

The user can model static and dynamic loads. Static load modelling in CPAT is done using the traditional method discussed in Chapter 4 described by Equations (4.1) and (4.2), however, CPAT multiplies the right hand side of the equation by $\left(1+\frac{\Delta f \beta}{100}\right)$ where Δf is the frequency deviation in Hz and β is the frequency characteristic index to include the frequency dependency of static loads.

For the case studies conducted, the frequency dependency of loads is not taken into

consideration, so Equations (4.1) and (4.2) are used unchanged.

7.4 LINEARIZATION IN CPAT

7.4.1 Linearization

The linearization in CPAT is analytical like MatNetEig. The linearization process is as described in chapter 2.

7.4.2 The S-Method

For very large power systems, the state matrix **A** matrix becomes very large. Attempts to solve such big matrices by conventional methods (full modal analysis) demand a memory capacity several times that of powerful existing computers and requiring unreasonably long execution times for analysis [37]. However, the S-Method is capable of handling very large systems by transforming the A matrix by Equation (7.1) into the S matrix to make the absolute values of a very well damped eigenvalue smaller and that of poorly damped eigenvalues large; thereby efficiently obtaining only eigenvalues that have large absolute values [12].

$$\begin{aligned} &\mathbf{S} = (\mathbf{A} + h\mathbf{I})(\mathbf{A} - h\mathbf{I})^{-1} \\ &\text{where } h \text{ is a positive real constant} \\ &\mathbf{I} \text{ is the identity matrix} \end{aligned} \tag{7.1}$$

The eigenvalue of the **A** matrix λ_{Ai} is related to that of the **S** matrix λ_{Si} by Equation (7.2) below [12]:

$$\lambda_{Si} = \frac{(\lambda_{Ai} + h)}{(\lambda_{Ai} - h)} \tag{7.2}$$

The geometric interpretation of Equation (7.2) is that the left-half of the complex eigenvalue plane is mapped onto to a unit circle centred at the origin as shown below in Figure 7.3 [12].

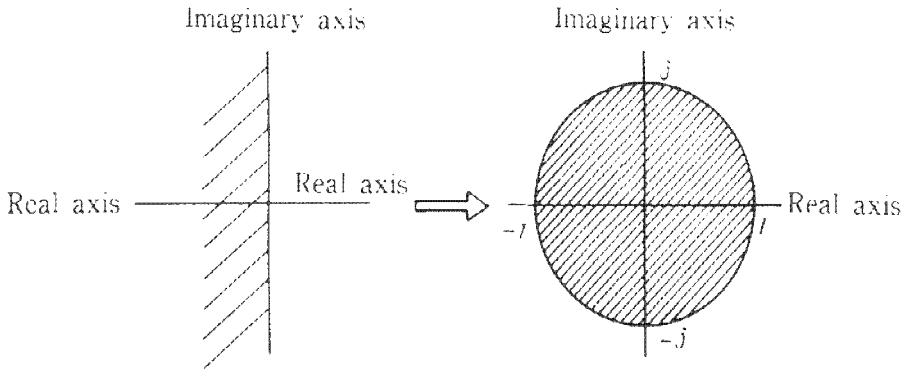

Figure 7.3: *The geometric interpretation of the S-matrix transformation [12].*

The S-Method then uses the largest absolute value of the eigenvalues of **S**, $\lambda_{S\max}$ to determine the stability of the system as follows:

$$\begin{aligned} &\text{Unstable if } |\lambda_{S\max}| > 1 \\ &\text{Stability limit if } |\lambda_{S\max}| = 1 \\ &\text{Stable if } |\lambda_{S\max}| < 1 \end{aligned} \tag{7.3}$$

The S-Method only calculates poorly damped eigenvalues. Because the S-Method does not perform full modal analysis (i.e. calculate all eigenvalues of **A**), it can handle systems of up to 1500 buses, 300 generators and 1800 branches.

7.4.3 Eigenvalue Calculation in CPAT

There are several approaches used in the calculation of eigenvalues. The S-method uses the Lanczos method approach [12]. According to [12] this method is best suited for obtaining several eigenvalues of a large matrix that is sparse. This approach proves most effective for the S-Method since the aim is to calculate several eigenvalues (those with a large absolute value) of the sparse S matrix [12]. The actual calculation of eigenvalues of the S-matrix employs the QR method and then the eigenvalues of A are obtained by Equation (7.2) [12].

7.5 SPECIAL FEATURES OF CPAT

- The user can build custom generator control system models using special blocks.
- The user can also use CPAT to optimize generator control system parameters for different load flow operating conditions. This uses eigenvalues sensitivity to give

the user a number of solutions from which the user can choose.

- The CPAT platform, POPONAS, is a graphical user interface that also allows the user to draw the network diagram. However, the user cannot enter system data on the one line diagram. Like the other two tools, data is input text files. The user must follow the sequence specified in the manual taking note of the column position of the input. Data is output in text files.

CHAPTER 8
System Models, Case Studies and Results

8.1 INTRODUCTION

In this chapter, the description of the two system models investigated, the case studies and the discussion of the simulation results are presented. The two system models used for the investigation are the single machine infinite bus system (SMIB) and the two-area four-generator system (2A4G). The small-disturbance stability of the two systems is investigated with the systems under the following excitation system control configurations:

- The system is under manual excitation control
- The excitation system is equipped with automatic voltage regulation (AVR)
- The excitation system is equipped with AVR and a power system stabilizer (PSS).

This chapter is divided into three sections. Section 8.2 presents the description of the two system models, Section 8.3 presents the case studies conducted and Section 8.4 presents the discussion of the simulation results that were obtained.

8.2 SYSTEM MODEL

8.2.1 The Single Machine Infinite Bus Test System (SMIB)

The system comprises a thermal generating station consisting of four 555MVA, 24kV, 60Hz units connected to a relatively large system, often referred to as an infinite bus in power systems, via a transmission line of impedance j0.65p.u. The four 555MVA units are lumped together into one 2220MVA generating unit. The line reactance is in per unit on a 2220MVA, 24kV base. In [1] the single machine infinite bus system comprises of a 1:1 transformer of impedance j0.15 in series with a transmission line of impedance j0.5. However, in the case studies conducted the transformer was lumped with the transmission line to an equivalent impedance of j0.65.

Because of the relative size of the system to which the generator is supplying power, dynamics associated with the generator will cause virtually no change in the voltage and frequency of the Thevenin's voltage that is used to represent the large system [1]. In power systems, a voltage source of constant voltage and frequency is referred to as an infinite bus.

The system model is shown in Figure 8.1. The system operating condition and generator dynamic data can be found in appendix A1.

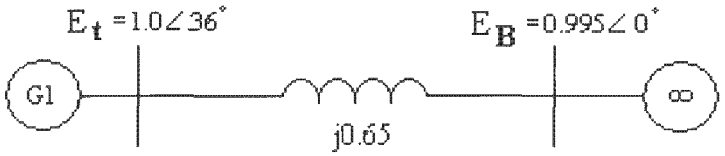

Figure 8.1: *The reduced single machine infinite bus test system [1]*

8.2.2 Small Signal Stability Analysis of the SMIB

The small signal stability analysis of the SMIB was the first study that was carried out using the three tools.

The small signal stability analysis of the SMIB was carried out with the synchronous machine represented by models of varying degrees of detail. The classical or second order model was used first and the model detail was increased to the sixth order taking into consideration the effects of the dynamics of the field circuit and the damper windings.

The system was studied in three different configurations of excitation system control:

- System under manual control with the generator represented by the classical model
- System under manual control with the generator represented by the sixth order model (detailed model)
- System with the generator represented by the detailed model equipped with an excitation system with automatic voltage regulation (AVR)
- System with the generator represented by the detailed model equipped with an excitation system with AVR and a power system stabilizer (PSS)

These investigations were carried out to investigate the capabilities of these simulation tools.

8.2.3 The Two-Area Four-Generator System (2A4G)

The system comprises two areas connected by a weak tie (a long transmission path).

- Area 1 comprises generators G1 and G2
- Area 2 comprises generators G3 and G4

Each area consists of two coupled 900MVA , 20kV , 60Hz synchronous generators. All the generator parameters are in per unit on their rated MVA and kV bases. The generator parameters of the two-area system can be found in Appendix A2 and the system is shown in Figure 8.2.

There are four step-up 20/230kV transformers with an impedance of $j0.15$p.u. on a 900MVA and 20/230kV base with an off-nominal ratio of 1.0. The transmission system nominal voltage is 230kV . The line lengths are identified in Figure 8.2. Line parameters are specified in per unit, on a 100MVA and 230kV base. Line parameters and system operating point data can be found in Appendix A2.

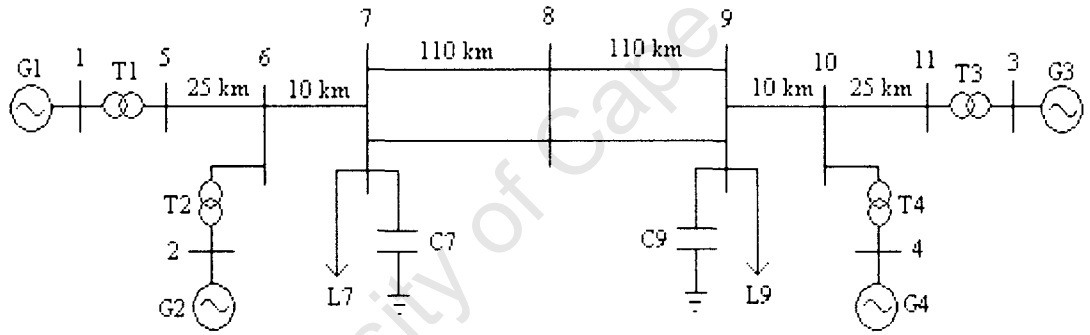

Figure 8.2: *Two-area four-generator test system [1].*

8.2.4 Small Signal Stability of the 2A4G

The 2A4G system exhibits local and inter-area oscillations. The different modes of oscillations were discussed in Section 2.6. The small signal stability analysis of the system is carried out with the generators represented by the detailed model in three operation modes as follows:

- System is under manual control
- System with all generators equipped with similar excitation systems with AVR
- System with all generators equipped with similar excitation systems with AVR

and PSSs

These cases were carried out to investigate the capabilities of these simulation tools in revealing the effects of the various factors associated with synchronous machines in small signal stability.

8.3 OVERVIEW OF CASE STUDIES

Analysis of systems having simple configurations like the SMIB discussed in this thesis is extremely useful for understanding the basic effects of different power system components like the AVR, PSS and the degree of detail of generator models and concepts of small-disturbance stability analysis [1].

The generator magnetic saturation was neglected for all the simulations that were carried out. The classical and the sixth order generator models were used for the simulations carried out on the single machine infinite bus (SMIB) system. Only the sixth order generator model was used for the simulations carried out on the 2A4G system. The loads in the 2A4G system were modelled as static loads as specified in [1].

8.3.1 The Single Machine Infinite Bus System (SMIB)

To investigate the small signal stability of the single machine infinite bus system, the following case studies were conducted:

Case 1	The generator is modelled with the classical model. With the system under manual control, the small-disturbance stability of the system is investigated
. **Case 2**	The generator of the SMIB is now modelled using the detailed sixth order model. The small-disturbance stability of the system under manual control is investigated.
Case 3	An exciter with AVR is added on to the generator of the system described in case 2 and the small-disturbance stability is investigated. Exciter data can be found in appendix A1.
Case 4	A power system stabilizer is added on the generator of the system described in case 3 and the small-disturbance stability of the system is investigated. Exciter and PSS data can be found in appendix A1.

8.3.2 The Two-Area Four-Generator System

For all the case studies conducted on this system, all the generators were modelled using detailed sixth order generator models.

Case 5	The system is under manual control. The small-disturbance stability is investigated.
Case 6	All generators in the system are equipped with excitation systems with AVR. The small-disturbance stability is investigated. For exciter data see appendix A2.
Case 7	All generators in the system are equipped with excitation systems with AVR and PSSs. The small-disturbance stability of the system is investigated.

8.4 SIMULATION RESULTS

8.4.1 The Single Machine Infinite Bus System

8.4.1.1 Frequency Domain Analysis

Case 1: SMIB with Classical Generator Model

Table 8.1 shows the eigenvalues calculated in CPAT, MatNetEig and PST. CPAT only outputs the real part of the eigenvalue and its frequency of oscillation. PST and MatNetEig output both the real and imaginary part of the eigenvalue, the frequency of oscillation and the damping ratio. The damping ratios for the results obtained in CPAT were calculated using MATLAB.

Table 8.1: Eigenvalues of the SMIB, generator modelled with the classical model

PST	MatNetEig	CPAT
0 ± j6.3861 ω_d = 1.0164 Hz ζ = 0	0 ± j6.390 ω_d = 1.0165 Hz ζ = 0	0 ± j6.3866 ω_d = 1.0165 Hz ζ = 0

In PST and MatNetEig the user can view participation factors. Using the participation factors, the user can determine which states participate in a particular mode. Table 8.2 shows the normalized participation factor magnitudes for the oscillatory mode. The participation factors obtained imply that the dominant

states are the speed and the angle. Therefore, this is a rotor angle (or electromechanical) mode of oscillation, and adding damping at the generator shaft will increase the damping of the mode.

Table 8.2: Normalized participation factor magnitudes

Generator	State	Normalized Participation Factor Magnitude
1	δ	1
1	ω	1

Case 2: SMIB with Sixth Order Generator Model (No AVR, Manual Control)

Table 8.3 shows the eigenvalues calculated in CPAT, MatNetEig and PST. The generator was modelled using the detailed sixth order model. There are in total six eigenvalues, but only the complex eigenvalues are dominant and these correspond to the local mode. As expected, higher order models exhibit better damping than lower order models since they include the effects of amortisseurs (dampers) [23]. CPAT uses the S-Method, which calculates a selection of eigenvalues but not all the eigenvalues of the system. Therefore, in the following tables of eigenvalues, the eigenvalues that were not output by CPAT are represented by "n/a".

Table 8.3: Eigenvalues of the SMIB, generator modelled with sixth order model (manual control)

PST	MatNetEig	CPAT
-0.5052	-0.0505	-0.0503
-1.7384	-1.7428	n/a
-0.2034 ± j6.4209 ω_d = 1.0219 Hz ζ = 0.0317	-0.2030 ± j6.7207 ω_d = 1.0696 Hz ζ = 0.0302	-0.24733 ± j6.4166 ω_d = 1.0212 Hz ζ = 0.0385
-22.304	-21.755	n/a
-36.409	-36.409	-36.403

n/a: result not output

Table 8.4 shows the normalized participation factor magnitudes obtained in PST and MatNetEig for the oscillatory mode. The participation factors obtained imply that the dominant states are the speed and the angle, therefore this is a rotor angle mode of oscillation.

Table 8.4: Normalized participation factor magnitudes

Generator	State	Normalized Participation Factor Magnitude
1	δ	1
1	ω	1
1	E'_q	0
1	Ψ''_d	0
1	E'_d	0
1	Ψ''_q	0

Case 3: SMIB with Sixth Order Generator Models with AVR

Table 8.5 shows the eigenvalues calculated in CPAT, MatNetEig and PST. The generator is modelled using the detailed sixth order model equipped with an exciter with AVR. Compared to the previous case, the eigenvalues increase by one because the generator now has a simplified AVR (first order). The results obtained from all three simulation tools show that adding on automatic excitation control to the system decreases the damping of the electromechanical modes, as can be seen by the positive real parts of the eigenvalues in the third row in Table 8.5. The other eigenvalues (including the complex eigenvalues) are well damped and are not of concern.

Table 8.5: Eigenvalues of the SMIB, sixth order model equipped with AVR

PST	MatNetEig	CPAT
-1.6465	**-1.651**	**n/a**
0.5673 ± j7.4397 **ω_d = 1.1841 Hz** **ζ = -0.076**	**0.5617 ± j7.3068** **ω_d = 1.1629 Hz** **ζ = -0.0766**	**0.5032 ± j7.3653** **ω_d = 1.1722 Hz** **ζ = -0.0682**
−17.042 ± j12.164 **ω_d = 1.936 Hz** **ζ = 0.8139**	**−17.036 ± j12.254** **ω_d = 1.9502 Hz** **ζ = 0.8118**	**n/a**
-22.114	**-21.562**	**n/a**
-54.199	**-54.201**	**n/a**

n/a: result not output

Table 8.6 shows normalized participation factor magnitudes obtained in PST and MatNetEig corresponding to the eigenvalues 0.5673±j7.4397 and 0.5617±j7.3068. The participation factors obtained imply that this is an electromechanical mode of oscillation. Table 8.6 shows that the field flux linkage also participates in this mode.

Table 8.6: Normalized participation factor magnitudes

Generator	State	Normalized Participation Factor Magnitude
1	δ	1
1	ω	1
1	E'_q	0.1749
1	Ψ''_d	0
1	E'_d	0
1	Ψ''_q	0
1	V_TR	0

Table 8.7 shows normalized participation factor magnitudes obtained with PST and MatNetEig corresponding to the eigenvalues −17.042±j12.164 and −17.036±j12.254. The participation factors obtained show that these eigenvalues are related to the exciter.

Table 8.7: Normalized participation factor magnitudes

Generator	State	Normalized Participation Factor Magnitude
1	[illegible]	0
1		0
1	E'_q	1
1	Ψ''_d	0.5365
1	E'_d	0
1	Ψ''_q	0
1	V_TR	0.6009

Case 4: SMIB, Sixth Order Generator Model, AVR + PSS

Table 8.8 shows the eigenvalues calculated in CPAT, MatNetEig and PST. The generator was modelled using the detailed sixth order model, equipped with an exciter with AVR and a PSS. The inclusion of the PSS (two sates) has increased the total number of eigenvalues by two. The results obtained from all three

simulation tools show that adding a PSS to the system increases the damping of the electromechanical mode. This mode corresponds to the eigenvalues in the fourth row of Table 8.8, where it can be seen that the real parts of these eigenvalues are negative.

Table 8.8: Eigenvalues of the SMIB, sixth order model equipped with AVR + PSS

PST	MatNetEig	CPAT
-0.742	-0.7355	n/a
-1.6328	-1.6276	n/a
-1.1461 ± j6.7626 ω_d = 1.076 Hz ζ = 0.1671	-1.1377 ± j6.7144 ω_d = 1.0686 Hz ζ = 0.1671	-1.1865 ± j6.8886 ω_d = 1.0964 Hz ζ = 0.1697
-13.264 ± j16.343 ω_d = 2.601 Hz ζ = 0.6302	-13.275 ± j16.386 ω_d = 2.6079 Hz ζ = 0.6295	n/a
-22.236	-21.689	n/a
-34.187	-34.182	-38.217
-54.308	-54.311	n/a

n/a: result not output

Table 8.9 shows normalized participation factor magnitudes obtained in PST and MatNetEig corresponding to these eigenvalues -1.1461±j6.7626 and -1.1377±j6.7144. The participation factors obtained imply that this is an electromechanical mode of oscillation.

Table 8.9: Normalized participation factor magnitudes

Generator	State	Normalized Participation Factor Magnitude
1	δ	1
1	ω	0.8028
1	E'_q	0.149
1	Ψ''_d	0
1	E'_d	0
1	Ψ''_q	0
1	V_TR	0
1	pss1	0
1	pss2	0.3059

Table 8.10 shows normalized participation factor magnitudes obtained in PST and MatNetEig corresponding to the eigenvalues -13.264±j16.343 and -13.275±j16.386. The participation factors obtained show that this mode of oscillation is associated with the excitation system.

Table 8.10: Normalized participation factor magnitudes for mode

Generator	State	Normalized Participation Factor Magnitude
1	δ	0
1	ω	0.2967
1	E'_q	1
1	Ψ''_d	0.3976
1	E'_d	0
1	Ψ''_q	0
1	V_TR	0.3935
1	pss1	0
1	pss2	0.3774

8.4.1.2 Time Domain Responses

In PST and MatNetEig, the user can perform a step response simulation to see the response of the system in the time domain. Figure 8.3 shows the time domain response of the system obtained in PST and MatNetEig. A 0.01pu step change was applied to the voltage reference input of the AVR. The unstable mode can be seen in the time domain. Figure 8.3 shows that oscillations start immediately *(although not visible in the Figure)* after the disturbance and are growing in amplitude.

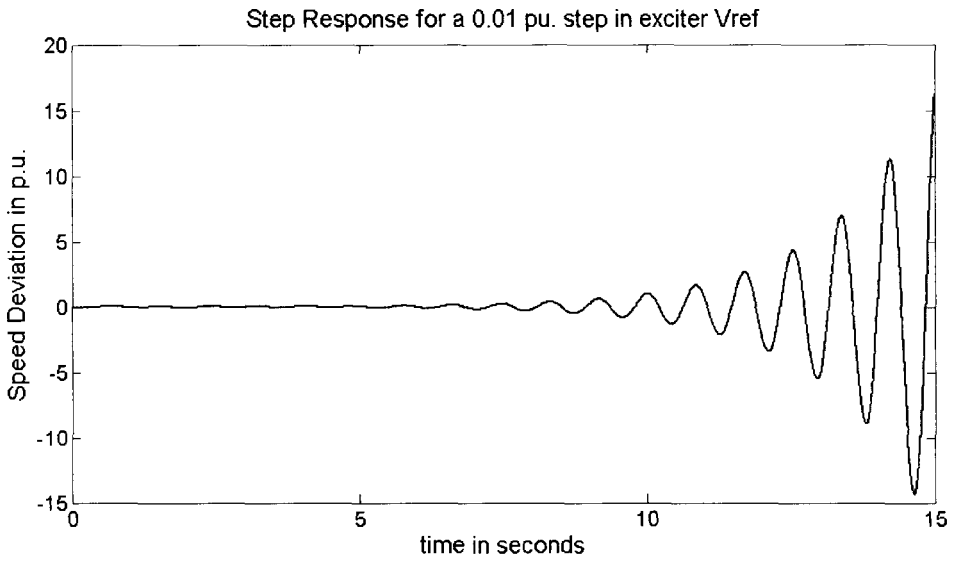

Figure 8.3: *Response of generator speed to a 0.01pu step change in Vref*

Figure 8.4 shows the time domain response of the system obtained in PST and MatNetEig whith PSS included. It can be seen from the figure that with the addition of the PSS, the system is stable. The oscillations are now damped within about 3 seconds.

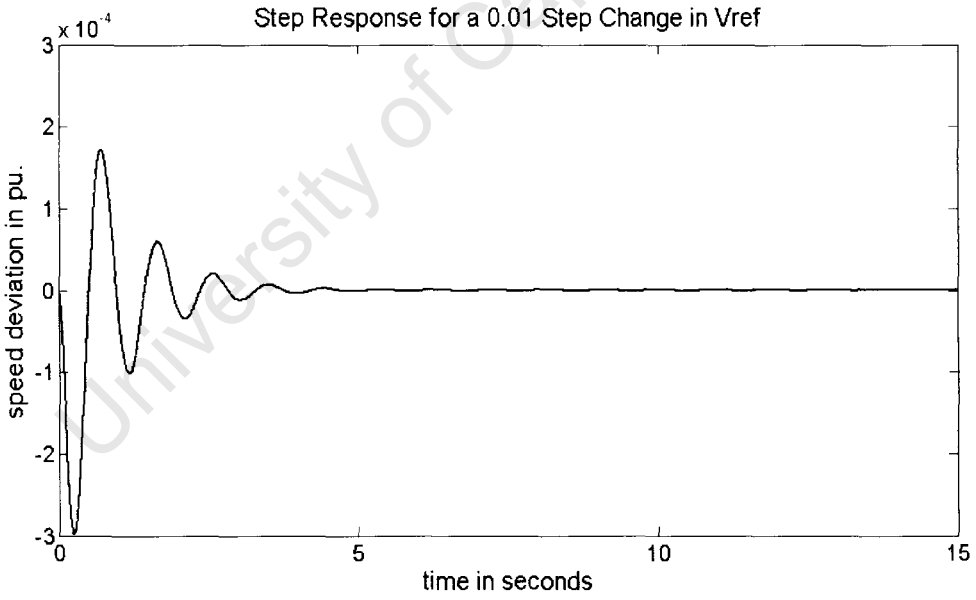

Figure 8.4: *Response of generator speed to a 0.01pu step change in Vref*

8.4. 2 The Two-Area Four-Generator System (2A4G)

8.4.2.1 Frequency Domain Analysis

Note that all generators were modelled using the sixth order model.

Case 5: 2A4G system under Manual Control

Table 8.11 shows the eigenvalues calculated in CPAT, MatNetEig and PST. It can be seen from the table that the system is stable. There are three electromechanical modes of oscillation. There is one inter-area mode associated with the eigenvalues -0.1225 ± j3.4225 and two local modes of oscillation associated with the eigenvalues -0.5802 ± j6.7894 and -0.5892 ± j6.9822, respectively.

Table 8.11: Eigenvalues, system under manual control

Mode	PST	MatNetEig	CPAT
Inter-area mode	**-0.1225 ± j3.4225** **ω_d = 0.5447 Hz** **ζ = 0.0358**	**-0.1225 ± j3.4225** **ω_d = 0.5447 Hz** **ζ = 0.0358**	**-0.1244 ± j3.4202** **ω_d = 0.5443 Hz** **ζ = 0.0364**
Area 1 local mode	**-0.5802 ± j6.7894** **ω_d = 1.1081 Hz** **ζ = 0.0851**	**-0.5802 ± j6.7894** **ω_d = 1.1081 Hz** **ζ = 0.0851**	**-0.6403 ± j6.7312** **ω_d = 1.0713 Hz** **ζ = 0.0947**
Area 2 local mode	**-0.5892 ± j6.9822** **ω_d = 1.1112 Hz** **ζ = 0.0841**	**-0.5892 ± j6.9822** **ω_d = 1.1112 Hz** **ζ = 0.0841**	**-0.6454 ± j6.9498** **ω_d = 1.1061 Hz** **ζ = 0.0925**

n/a: result not output

Table 8.12 shows the normalized participation factor magnitudes obtained in PST and MatNetEig for the inter-area mode. From the participation factors obtained it can be seen that all generators in the system participate in the inter-area mode.

Table 8.12: Normalized participation factor magnitudes

Generator	State	Normalized Participation Factor Magnitude
1	δ	0.4406
1	ω	0.4406
1	E'_q	0
1	Ψ''_d	0
1	E'_d	0
1	Ψ''_q	0
2	δ	0.2531
2	ω	0.2531
2	E'_q	0
2	Ψ''_d	0
2	E'_d	0
2	Ψ''_q	0
3	δ	1
3	ω	1
3	E'_q	0
3	Ψ''_d	0
3	E'_d	0
3	Ψ''_q	0
4	δ	0.7503
4	ω	0.7503
4	E'_q	0
4	Ψ''_d	0
4	E'_d	0
4	Ψ''_q	0

In PST and MatNetEig it is possible for the user to access right eigenvectors and view compass plots of the right eigenvectors. Figure 8.5 shows the compass plot of the right eigenvector components associated with speed changes. It can be seen from the figure that speed changes (oscillations) of the generators in area 1 (G1 and G2) are out of phase (almost 180 degrees) with those of generators in area 2 (G3 and G4) which implies that in the inter-area mode, generators in area 1 swing against those in area 2.

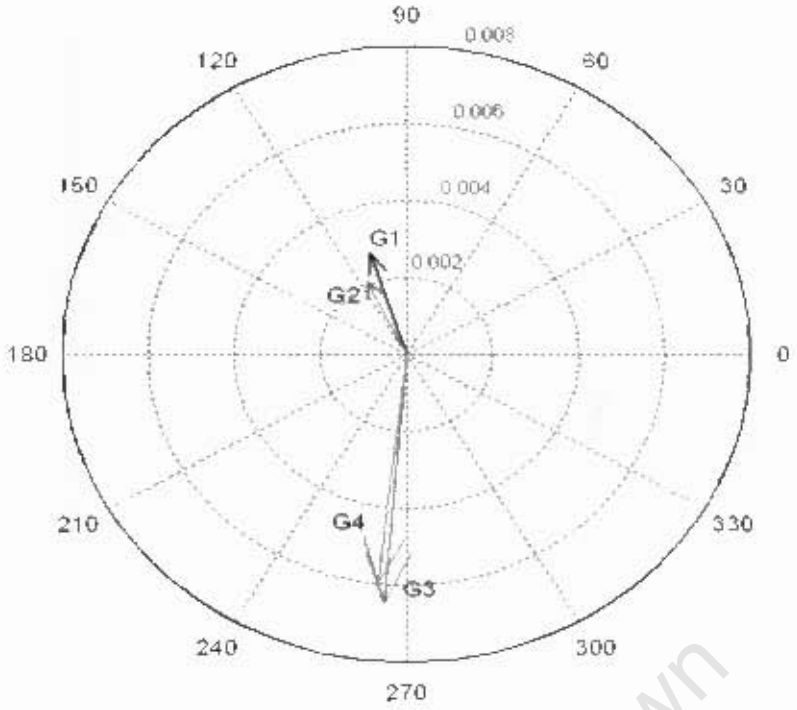

Figure 8.5: Compass plot of rotor speed right eigenvector components for the inter-area mode

Table 8.13 shows the normalized participation factor magnitudes obtained in PST and MatNetEig for the area 1 local mode. From the participation factors obtained, it can be seen that the generators in area 1 (G1 & G2) participate in the area 1 local mode associated with the eigenvalues -0.5802 + j6.7894.

Table 8.13: Normalized participation factor magnitudes

Generator	State	Normalized Participation Factor Magnitude
1	δ	0.80161
1	ω	0.80161
1	E'_q	0
1	Ψ''_d	0
1	E'_d	0
1	Ψ''_q	0
2	δ	1
2	ω	1
2	E'_q	0
2	Ψ''_d	0
2	E'_d	0
2	Ψ''_q	0
3	δ	0
3	ω	0
3	E'_q	0
3	Ψ''_d	0
3	E'_d	0

Generator	State	Normalized Participation Factor Magnitude
3	Ψ''_q	0
4	δ	0
4	ω	0
4	E'_q	0
4	Ψ''_d	0
4	E'_d	0
4	Ψ''_q	0

Figure 8.6 shows the compass plot of the right eigenvector components associated with speed changes. It can be seen from the figure that speed changes of generator G1 in area 1 are out of phase with those of generator G2 in area 1 which implies that for the area 1 local mode, G1 swings against G2. Table 8.13 shows that the participation of G3 and G4 in the area 1 local mode is negligible.

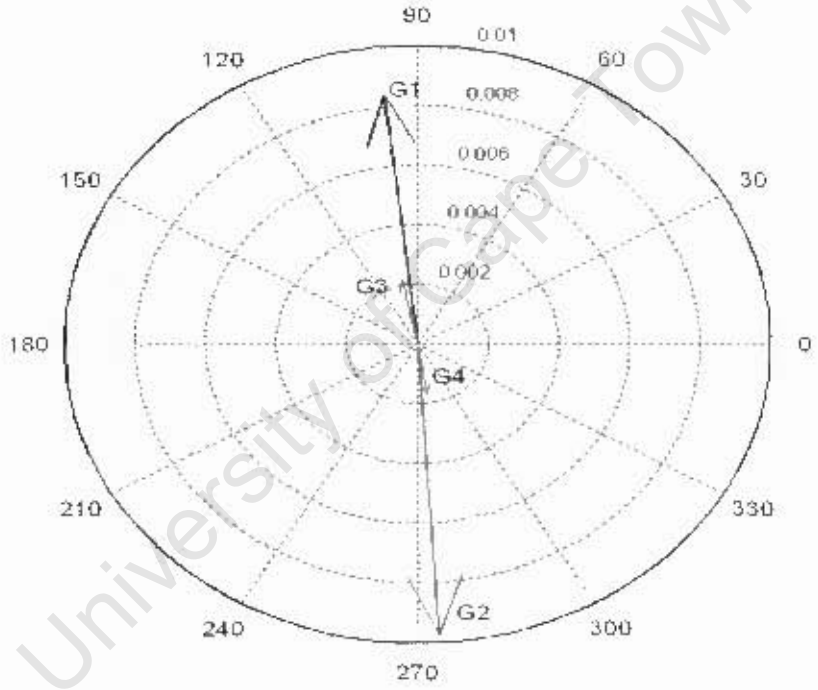

Figure 8.6: *Compass plot of rotor speed right eigenvector components for the area-1 local mode*

Table 8.14 shows the normalized participation factor magnitudes obtained in PST and MatNetEig for the area 2 local mode. From the participation factors obtained, it can be seen that the generators in area 2 (G3 & G4) participate in the area 2 local mode associated with the eigenvalues -0.5892 ± j6.9822.

Table 8.14: Normalized participation factor magnitudes

Generator	State	Normalized Participation Factor Magnitude
1	δ	0
1	ω	0
1	E'_q	0
1	Ψ''_d	0
1	E'_d	0
1	Ψ''_q	0
2	δ	0
2	ω	0
2	E'_q	0
2	Ψ''_d	0
2	E'_d	0
2	Ψ''_q	0
3	δ	0.73959
3	ω	0.73959
3	E'_q	0
3	Ψ''_d	0
3	E'_d	0
3	Ψ''_q	0
4	δ	1
4	ω	1
4	E'_q	0
4	Ψ''_d	0
4	E'_d	0
4	Ψ''_q	0

Figure 8.7 shows the compass plot of the right eigenvector components associated with speed changes. It can be seen from the figure that speed changes of generator G3 in area 2 are out of phase with those of generator G4 in area 2, which implies that for the area 2 local mode, G3 swings against G4. Table 8.14 shows that the participation of G1 and G2 in the area 2 local mode is negligible.

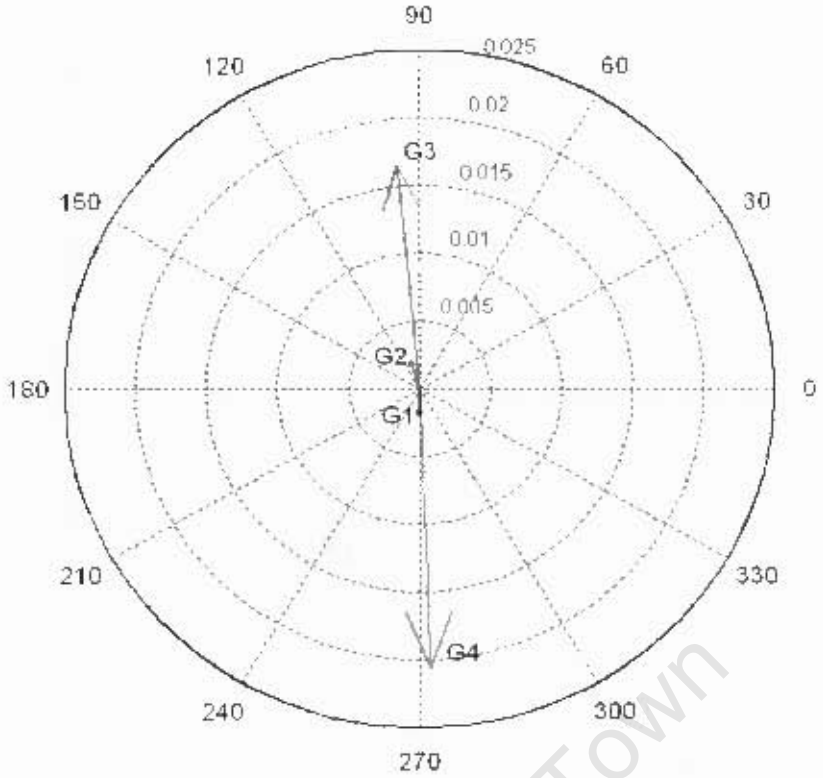

Figure 8.7: Compass plot of rotor speed right eigenvector components for area-2 local mode

Case 6: System with AVR without PSS

Table 8.15 shows the eigenvalues calculated in CPAT, MatNetEig and PST. It can be seen from the table that the addition of the AVR to the exciter destabilised the inter-area mode. However, the damping of the local modes has increased slightly.

Table 8.15: Eigenvalues system with AVR only

Mode	PST	MatNetEig	CPAT
Inter-area mode	0.0069 ± j3.8440 ω_d = 0.6118 Hz ζ = -0.0018	0.0155 ± j3.8495 ω_d = 0.6127 Hz ζ = -0.0040	0.0102 ± j3.8025 ω_d = 0.60518 Hz ζ = -0.0027
Area 1 local mode	-0.6601 ± j7.1667 ω_d = 1.1406 Hz ζ = 0.0917	-0.6428 ± j7.088 ω_d = 1.1281 Hz ζ = 0.0903	n/a
Area 2 local mode	-0.6539 ± j7.3675 ω_d = 1.1726 Hz ζ = 0.0884	-0.6513 ± j7.3647 ω_d = 1.1721 Hz ζ = 0.0881	n/a

n/a: result not output

Case 7: System with AVR and PSS

Table 8.16 shows the eigenvalues calculated in CPAT, MatNetEig and PST. The addition of the PSS to the system has stabilized the inter-area mode as can be seen by the positive values of the damping ratios.

Table 8.16: Eigenvalues, system with AVR + PSS

Mode	PST	MatNetEig	CPAT
Inter-area mode	**-0.5467 ± j3.826** **ω_d = 0.6089 Hz** **ζ = 0.1415**	**-0.5234 ± j3.8108** **ω_d = 0.6065 Hz** **ζ = 0.1361**	**-0.6015 ± j3.775** **ω_d = 0.6012 Hz** **ζ = 0.1573**
Area 1 local mode	**-2.1334 ± j8.2070** **ω_d = 1.3062 Hz** **ζ = 0.2516**	**-2.0862 ± j8.2422** **ω_d = 1.3118 Hz** **ζ = 0.2454**	**n/a**
Area 2 local mode	**-2.1947 ± j8.5226** **ω_d = 1.3564 Hz** **ζ = 0.2494**	**-2.1974 ± j8.5194** **ω_d = 1.3559 Hz** **ζ = 0.2498**	**n/a**

n/a: result not output

8.4.2.1 Time Domain Analysis

Case 6: System with AVR without PSS

A step response simulation was carried out in PST and MatNetEig to see the time domain response of the system. A 0.01 pu step disturbance was applied to the AVR reference voltage Vref. The inter-area mode can be seen in the time domain response of the system depicted in Figure 8.8. The system is unstable with a frequency of oscillation of about 0.61 Hz.

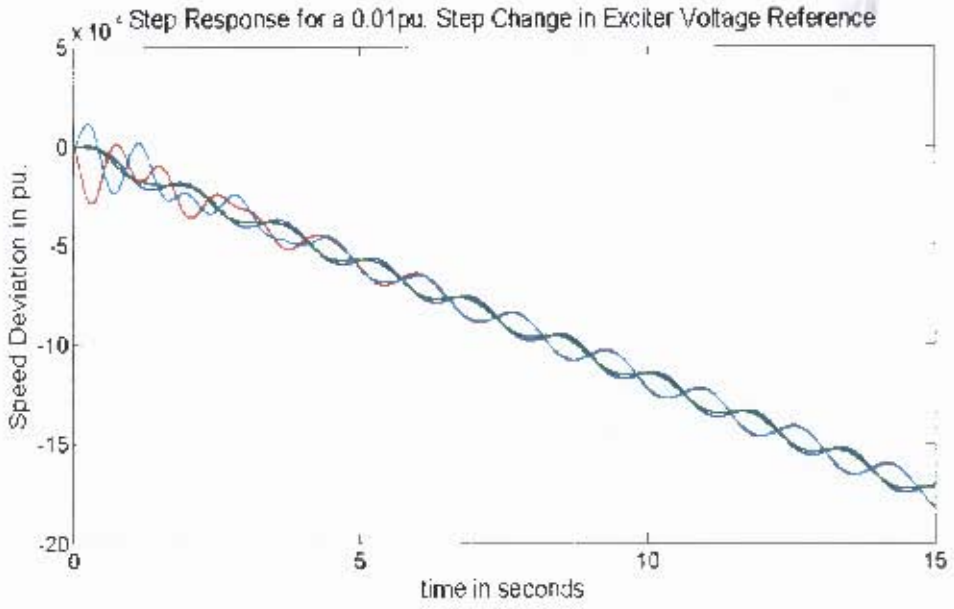

***Figure 8.8**: Step response of the system with AVR to a 0.01pu step change in Vref*
G1 - green, G2 – blue, G3 – red, G4 – Cyan

The frequency of oscillation in the time domain was calculated to be about 0.611Hz. This does not deviate far from the frequency domain results. The frequency was calculated by taking two points on the curve from MATLAB over one complete cycle. This can easily be done in MATLAB by moving the mouse pointer along the curve.

Case 7: System with AVR and PSS

A step response simulation was carried out in PST and MatNetFig to see the time domain response of the system. The inter-area mode can be seen in the time domain response of the system depicted in Figure 8.9. The system is stable with a settling time of about 6sec.

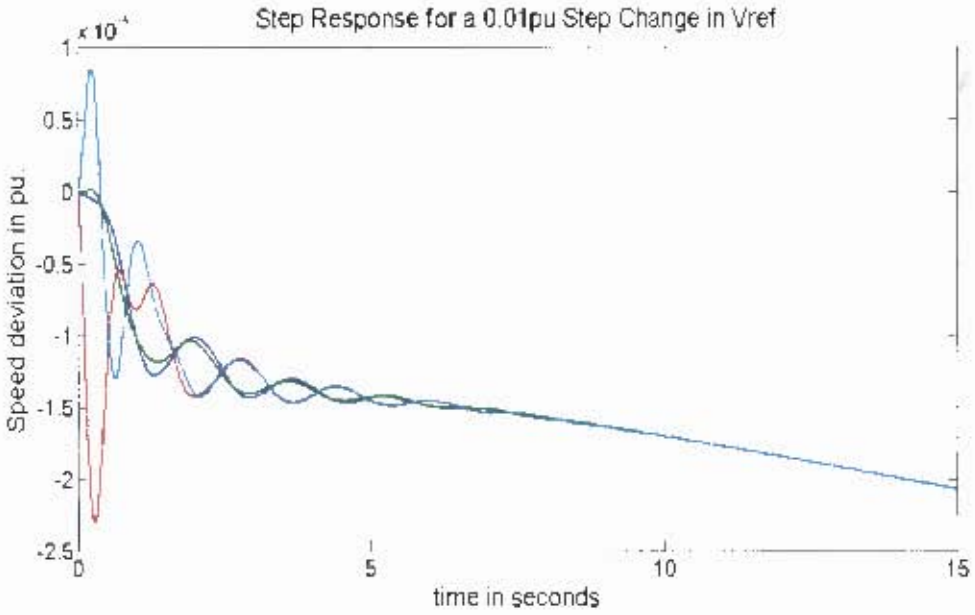

Figure 8.9: Step response of the system with AVR and PSS to a 0.01pu step change in Vref

The frequency of oscillation in the time domain was calculated to be about 0.61Hz, which closely matches the frequency domain results.

8.5 DISCUSSIONS OF THE SIMULATION RESULTS

Case 1:

For this case, the value of the frequency of oscillation obtained with MatNeiEig is the identical as that obtained with CPAT. However, MatNeteig gives a slightly higher value which is about 0.01% bigger value than that of PST. This difference is very small and can be neglected. It can be argued that for this case the results obtained from the three simulation tools are identical.

Case 2:

The difference in frequency between CPAT and PST is about 0.07%, which is negligible. MatNetEig gives a frequency which is about 4.77% lower than that obtained with PST and CPAT.

Case 3:

The difference in frequency between MatNetEig and PST is about 1.8%. The difference in frequency between CPAT and PST is about 1%.

Case 4:

The difference in frequency between MatNetEig and PST is about 0.7%. The difference in frequency between CPAT and PST is about 1.9%.

Case 5:

For the inter-area mode of oscillation, the frequency obtained in MatNetEig and PST is the same. The difference in frequency between CPAT and PST is about 0.07%.

For the area-1 local mode of oscillation, the frequency obtained in MatNetEig and PST is the same. The difference in frequency between CPAT and PST is about 3.3%.

For the area-2 local mode of oscillation, the frequency obtained in MatNetEig and PST is the same. The difference in frequency between CPAT and PST is about 0.5%.

Case 6:

For the inter-area mode of oscillation, the difference in frequency between MatNetEig and PST is about 0.15%. The difference in frequency between CPAT and PST is about 1.08%.

For the area-1 local mode of oscillation, the difference in frequency between MatNetEig and PST is about 1.9%.

For the area-2 local mode of oscillation, the difference in frequency between MatNetEig and PST is about 0.04%.

Case 7:

For the inter-area mode of oscillation, the difference in frequency between MatNetEig and PST is about 0.4%. The difference in frequency between CPAT and PST is about 1.26%.

For the area-1 local mode of oscillation, the difference in frequency between MatNetEig and PST is about 0.43%.

For the area-2 local mode of oscillation, the difference in frequency between MatNetEig and PST is about 0.04%.

SUMMARY OF CAPABILITIES

Table 8.24 summarizes capabilities of the three simulation tools. The format of table 8.24 was adopted from [7].

Table 8.24: Summary of capabilities

		PST	MatNetEig	CPAT
Components models	Generator models (order)	2nd, 4th, 6th	2nd, 6th	2nd, 3rd, 4th, 5th, 6th
	Excitation system models	4 types	all standard IEEE	11 kinds, custom user built
	PSS models	1 type	1 type	4 kinds, custom user built
	Transmission line	pi-model	pi-model	pi-model, T-type, distributed parameters
	Load models	Polynomial (ZIP)	Polynomial (ZIP)	Exponential
Solution methodology	Linearization of system equations	Numerical	Analytical	Analytical
	Perturbation size* (*for numerical linearization)	Automatic		
	Eigenvalue calculation method	QR	QR	QR
	Modal analysis	full	full, partial	partial (S-method)
Software flexibility	Data input	Matrices in MATLAB	Matrices in MATLAB	Notepad file
	Data output	Matrices in MATLAB	Matrices in MATLAB	Notepad file
	Accessibility of system matrices	A, B, C and D	A, B, C and D	Information not available
	Eigenvectors	Right and left	Right and left	Information not available
	Participation factors	Available	Available	Information not available

PST is good for modelling small systems as it can only handle systems with up to 200 states. The library of pre-programmed excitation control system models is limited. The user can choose either a speed or a power input PSS. PST offers a quick command for performing time domain simulations on the linearized system. System variables are easily accessible in PST.

MatNetEig can model much bigger systems than PST. MatNetEig can model systems with over a 1000 states because it uses partial modal analysis. MatNetEig has a library of all standard IEEE excitation control system models. The user can choose between a power and a speed input PSS. System variables are easily accessible.

CPAT can model systems of up to 300 generators, 1500 nodes (buses) and 1800 branches (interconnections). CPAT has 11 kinds of AVRs and 4 kinds of PSSs pre-programmed however, it is also possible for the user to custom build an excitation control system using component blocks. The user has a choice between a speed, power or bus frequency as an input to the PSS. Using component blocks, it is possible for a user to build a multi-input PSS. With this package it also possible to perform excitation control system optimization using eigenvalue sensitivity analysis. More information on this subject can be found in [12], [15].

CHAPTER 9
Conclusions and Recommendations

Choosing which simulation package is best depends on the needs of the consumer. The objective of this thesis was to investigate the capabilities of the three simulation tools for small-disturbance angle stability analysis. The two MATLAB packages proved to be easier to work with because of the detailed user manuals, however CPAT proved to be the most practical in terms of the flexibility it provides to the users for modelling custom generator controls using special blocks.

9.1 CONCLUSIONS

PST in the author's view would be a good tool for teaching power systems as the documentation for PST is very detailed and the user has access to the source code used to make the software. This makes it easier for the teacher to explain the methods used by the software for various calculations. All internal system variables used in the calculations are easily accessible in MATLAB. PST can also run transient stability simulations, although simulating a real system in PST could be limited by the fact that it has no pre-programmed standard IEEE power system component model libraries and that it can only handle systems of up to 200 states.

The advantages of PST mentioned above can also be said for MatNetEig. However, MatNetEig is superior for modelling large systems. MatNetEig can handle larger systems than PST, up to systems over 1000 states for partial modal analysis. In addition, MatNetEig is more practical, because it comes with a library of pre-programmed IEEE excitation system models, to use to simulate real systems where these standard models are applicable.

One disadvantage is that MatNetEig is limited for small-signal stability studies as it cannot perform transient stability simulations.

With CPAT, the user can do small-disturbance and transient stability studies (calculation of eigenvalues) and it does come with pre-programmed standard IEEE power system

component model libraries. However, CPAT is more flexible because it offers special blocks and the user can build custom excitation system control models to match the real system being simulated, since real systems may not exactly match standard IEEE library models. The main differences between CPAT and the other two simulations tools is that it can handle large systems (more than 3000 states) because it employs the S-method which calculates only dominant eigenvalues.

CPAT comes with more features than the other two MATLAB packages. For example, it can be used for excitation system control optimization for small-disturbance stability enhancement and excitation system optimization for different load flow conditions but this was not within the scope of this thesis. The main problem with CPAT is the documentation. This is not as good when compared to PST and MatNetEig documentation.

The capabilities of the three simulation tools have been discussed. It is not easy to deduce which tool is best as it would largely depend on the user's needs and application.

9.2 RECOMMENDATIONS

It would be of great help to the users of power system simulation tools if study committees could be setup with computer engineering experts to:

- Draw up standards that simulation tools should meet in the different areas of specialisation. It could also help if tools that come into the market go through rigorous tests for validation using real power systems.
- Describe in detail the output required by the user and to differentiate between mandatory requirements and optional extra features.
- Grade the tools in terms of what they offer, so that a user wanting to run simple eigenvalue calculations of small systems would not run the risk of buying expensive simulation tools capable of handling very large systems, if that was not required.

As for PST and MatNetEig, it would be better if it was possible to view the network diagram the user is simulating as in CPAT. There is a lot of room for improvement in CPAT documentation, particularly if it had examples like PST and MatNetEig.

REFERENCES

[1] P. Kundur, *Power System Stability and Control*, New York: McGraw-Hill, 1994.

[2] IEEE/CIGRE Joint Task Force on Stability Terms and Definitions, "Definition and Classification of Power System Stability", IEEE Transactions on Power Systems, Vol 19, No. 2, May 2004.

[3] System Oscillations Working Group, "Inter-Area Oscillations in Power Systems", IEEE Power Engineering Society, 95 TP 101, October 1994.

[4] Kaberere, K.K., K.A. Folly, M. Ntombela, and A.I. Petroianu. "Comparative Analysis and Numerical Validation of Industrial-Grade Power System Simulation Tools: Application to Small-Signal Stability", Proceedings of the 15th PSCC, Liege, Belgium, August 22-26, 2005.

[5] M. Ntombela, K.K. Kaberere, K.A. Folly, A.I. Petroianu, "An Investigation into the Capabilities of MATLAB Power System Toolbox for Small Signal Stability Analysis", IEEE Power Engineering Society, Inaugural 2005 Conference and Exposition in Africa, July 11-15 UKZN 2005.

[6] M. Ntombela, A. Folly, "An Investigation into the Capabilities of MatNetEig for Small Signal Stability Analysis", Australasian Universities Power Engineering Conference, Hobart, Tasmania, 25 – 28 September, 2005.

[7] Kaberere, K.K., M. Ntombela, K.A. Folly, and A.I. Petroianu. "Comparison of Industrial-Grade Analytical Tools Used in Small-Signal Stability Assessment", Proceedings of the AUPEC 2005, Hobart, Tasmania, Australia, September 25-28, vol. 1, pp.147-152.

[8] G. Rogers, *Power System Oscillations*, Kluwer Academic Publishers, 2000.

[9] P. Kundur, G.J. Rogers, D.Y. Wong, L. Wang, M.G. Lauby, "A Comprehensive Computer Program Package for Small Signal Stability of Power Systems", IEEE Transactions on Power Systems, Vol. 5, No 4, November 1990, pp 1076-1083.

[10] J. G. Slootweg, J. Persson, A. M. van Voorden, G. C. Paap ,W. L. Kling, "A Study of the Eigenvalue Analysis Capabilities of Power System Dynamics Simulation Software", 14th PSCC, Sevilla, 24th – 28th June, 2002

[11] K. R. Padiyar, *Power System Dynamics: Stability and Control*, John Wiley & Sons, 1996.

[12] Power System Stability Group approved on 30 March 1990, *CRIEPI Report Integrated Analysis Software for Bulk Power System Stability*, Central Research Institute of Electric Power Industry, July 1991

[13] Kaberere, KK *Assessment of Five Industrial-grade Power System Simulation Tools: Variations in Modeling and Algorithmic Factors Impacting on Small-signal Stability Results*, Ph.D. Thesis, University of Cape Town, Dec. 2006.

[14] M. Braee, *Control Theory for Electrical Engineers*, UCT Press, 1994.

[15] Kenji Yoshimura, Naoyuki Uchida, "Optimization Method of P + ω PSS Parameters for Stability and Robustness Enhancement in a Multimachine Power System", Electrical Engineering in Japan, Vol. 131, No. 1, 2000, Translated from Denki Gakkai Ronbunshi, Vol. 118-B, No. 11, November 1998, pp. 1312-1320.

[16] G.C. Verghese, I.J. Perez-Arriaga, F.C. Schwepe, "Selective Modal Analysis with Application to Electric Power Systems, Part I and Part II", IEEE Trans. Vol. PAS-101, No.9, pp. 3117-3134, September 1982.

[17] M. Klein, G.J. Rogers, P. Kundur, "A Fundamental Study of Inter-Area Oscillations in Power Systems", IEEE Transactions on Power Systems, Vol. 6, No 3, August 1991, pp 914 – 921.

[18] G.J. Rogers, "Fundamental Aspects of Low Frequency Inter-Area Oscillations", published in 95 TP1, Inter-Area Oscillations in Power Systems by the System Oscillations Working Group

[19] Joe H. Chow, "Analytical Methods for Studying of Inter-Area Oscillations", published in 95 TP1, Inter-Area Oscillations in Power Systems by the System Oscillations Working Group.

[20] V. Vittal, N. Bhatia, A.A. Fouad, "Analysis of the Inter-Area Mode Phenomenon in Power Systems Following Large Disturbances", IEEE Transactions on Power Systems, Vol. 6, No 4, November 1991, pp 1515 – 1521.

[21] P.M. Anderson, "Power System Oscillation Summary of Utility Experience", published in 95 TP1, Inter-Area Oscillations in Power Systems by the System Oscillations Working Group

[22] "IEEE Guide for Synchronous Generator Modelling Practices in Stability Analysis", IEEE Std 1110-1991.

[23] E. Johansson et al., "Location of Eigenvalues Influenced by Different Models of Synchronous Machines", presented at the sixth IASTED International Conference Power and Energy Systems, May 13-15, 2002, Marina del Rey, California, USA.

[24] K.K. Kaberere, K.A. Folly and A.I. Petroianu, "Assessment of Commercially Available Software Tools for Transient Stability: Experience Gained in an Academic Environment", IEEE Africon 2004, 15 – 17 September 2004, volume 02, pp 711-716

[25] P. M. Anderson, A. A. Fouad, *Power System Control and Stability,* IEEE Press, 2nd edition, 2003

[26] http://www.eagle.ca/~cherry/pst.htm

[27] Joe Chow, Cherry Tree Scientific Software, "Power System Toolbox Version 2.0 Dynamic Tutorial and Functions" 1991-2003

[28] Joe Chow, Cherry Tree Scientific Software, "Power System Toolbox Version 2.0 Load Flow Tutorial and Functions" 1991-2003

[29] Cherry Tree Scientific Software, "Linearized Analysis of Power System Dynamics" 1997-2005

[30] http://www.eagle.ca/~cherry/index.htm

[31] http://www.eagle.ca/~cherry/rogers.htm

[32] http://www.eagle.ca/~cherry/MatNetEig.htm

[33] http://www.eagle.ca/~cherry/MATNETFLOW.htm

[34] Cherry Tree Scientific Software, "Generator Classes and Functions in MatNetEig" 1997-2005

[35] Cherry Tree Scientific Software, "Excitation System Models in MatNetEig" 1997-2004

[36] Cherry Tree Scientific Software, "MatNetEig Small Signal Stability Functions" 1997-2004

[37] Power Systems Department, Central Research Institute of Electric Power Industry, "User's Guide for the Analytical System for Power System Stability", February 2002

[38] Denryoku Computing Centre, "POPONAS for Windows User's Guide", 1985.

[39] T.M. Rakharebe, "PSS Optimization using the Eigenvalue Technique", 4th year thesis project, University of Cape Town, 2005

[40] Cherry Tree Scientific Software, "State Space Objects and Functions, Manual and Tutorial" 1997-2004

[41] Cherry Tree Scientific Software, "Using MatNetFlow" 1997-2004

[42] Cherry Tree Scientific Software, "Coherency in Interconnected AC Systems" 1999-2004

[43] Cherry Tree Scientific Software, "MatNetFlow Graphical User Interface" 1997-2005

APPENDICES

APPENDIX A

A1. THE SINGLE MACHINE INFINITE BUS SYSTEM

Network reactances are in per unit on a 2220 MVA, 24 kV base.

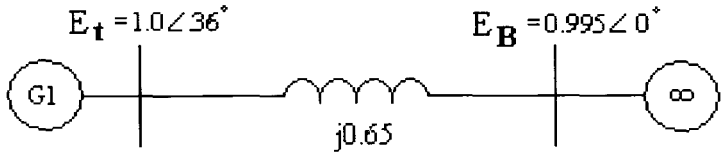

Generator Data on a 2220 MVA, 24kV base.

$X_d = 1.81$	$X_q = 1.76$	$X_l = 0.15$
$X'_d = 0.30$	$X'_q = 0.65$	$R_a = 0.003$
$X''_d = 0.23$	$X''_q = 0.25$	$H = 3.5$
$T'_{do} = 8.0$ s	$T'_{qo} = 1.0$ s	$K_D = 0$
$T''_{do} = 0.03$ s	$T''_{qo} = 0.07$ s	

Exciter and PSS Data

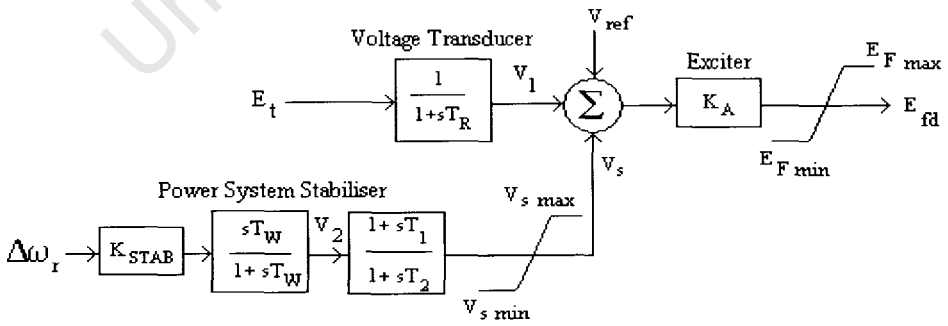

T_R=0.02s, K_A=200

K_{STAB}=9.5 T_W=1.4s T_1=0.154s T_2=0.033s

A2. THE TWO-AREA FOUR-GENERATOR SYSTEM

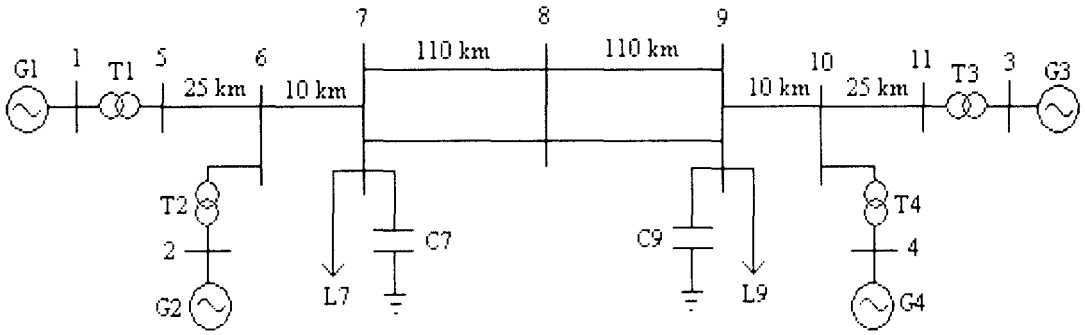

Generator data

Base: 900 MVA, 20 kV, 60 Hz

X_d = 1.8 X'_d = 0.3 X''_d = 0.25 A_{sat} = 0.015

X_q = 1.7 X'_q = 0.55 X''_q = 0.25 B_{sat} = 9.6

X_l = 0.2 T'_{do} = 8.0 s T''_{do} = 0.03 s ψ_{T1} = 0.9

R_a = 0.0025 T'_{qo} = 0.4 s T''_{qo} = 0.05 s K_D = 0

H = 6.5 (for G1 and G2) H = 6.175 (for G3 and G4)

Transmission lines

Base: 100MVA, 230 kV

r = 0.0001 pu/km xL = 0.001 pu/km bC = 0.00175 pu/km

Transformers

Rating: 900 MVA, 20/230 kV, X = j0.15 pu

Operating point set by the load flow

G1	P = 700 MW	Q = 185 MVAr	Vt = 1.03∠20.2°
G2	P = 700 MW	Q = 235 MVAr	Vt = 1.01∠10.5°
G3	P = 719 MW	Q = 176 MVAr	Vt = 1.03∠-6.8°
G4	P = 700 MW	Q = 202 MVAr	Vt = 1.01∠-17.0°
Bus 7	PL = 967 MW	QL = 100 MVAr	QC = 200 MVAr
Bus 9	PL = 1767 MW	QL = 100 MVAr	QC = 350 MVAr

Exciter and PSS Data

TR=0.01s, KA=200

KSTAB=20 TW=10s T1=0.05s T2=0.02s T3=3.0s T4=5.4s